Expert Systems With Applications 222 (2023) 119808

Contents lists available at ScienceDirect

Expert Systems With Applications

journal homepage: www.elsevier.com/locate/eswa

Designing porthole aluminium extrusion dies on the basis of eXplainable Artificial Intelligence

Juan Llorca-Schenk [a,*], Juan Ramón Rico-Juan [b], Miguel Sanchez-Lozano [c]

[a] Department of Graphic Expression, Composition and Projects, University of Alicante, Carretera San Vicente del Raspeig s/n, 03690 San Vicente del Raspeig (Alicante), Spain
[b] Department of Software and Computing Systems, University of Alicante, Carretera San Vicente del Raspeig s/n, 03690 San Vicente del Raspeig (Alicante), Spain
[c] Department of Mechanical Engineering and Energy, Miguel Hernandez University, Avenida de la Universidad, s/n., 03202 Elche (Alicante), Spain

ARTICLE INFO

Keywords:
Aluminium extrusion
Machine learning
Die design
Explainable machine learning
Hollow profile
Porthole

ABSTRACT

This paper shows the development of a tool with which to solve the most critical aspect of the porthole die design problem using a predictive model based on machine learning (ML). The model relies on a large amount of geometrical data regarding successful porthole die designs, information on which was obtained thanks to a collaboration with a leading extrusion company. In all cases, the dies were made of H-13 hot work steel and the billet material was 6063 aluminium alloy. The predictive model was chosen from a series of probes with different algorithms belonging to various ML families, which were applied to the analysis of geometrical data corresponding to 596 ports from 88 first trial dies. Algorithms based on the generation of multiple decision trees together with the boosting technique obtained the most promising results, the best by far being the CatBoost algorithm. The explainability of this model is based on a post-hoc approach using the SHAP (SHapley Additive exPlanations) tool. The results obtained with this ML-based model are notably better than those of a previous model based on linear regression as regards both the R^2 metric and the results obtained with the application examples. An additional practical advantage is its explainability, which is a great help when deciding the best way in which to adjust an initial design to the predictive model. This ML-based model is, therefore, an optimal means to integrate the experience and know-how accumulated through many designs over time in order to apply it to new designs. It will also provide an aid in generating the starting point for the design of high-difficulty dies, in order to minimise the number of FEM (finite element method) simulation/correction iterations required until an optimal solution is achieved. It is not aimed to eliminate FEM simulation from the design tasks, but rather to help improve and accelerate the whole process of designing porthole dies. The work presented herein addresses a validation model for a very common porthole die typology: four cavity and four port per cavity dies for 6xxx series aluminium alloys. However, a wide range of research regarding the generalisation of this model or its extension to other porthole die typologies must still be carried out.

1. Introduction

The use of lightweight materials and the improving of their forming processes lead to energy savings and reduced emissions. Aluminium alloys, whose favourable properties such as their low density, high corrosion resistance, easy formability… are superior to those of other materials, are widely used in a variety of industries. The need to reduce the weight of parts has also led to an increasing demand for the production of porthole extrusion dies with which to manufacture profiles with hollow cross-sections characterised by complex thin-walled geometries (Xue et al., 2018).

Furthermore, 6xxx series aluminium alloys make up more than half of all extrusion products. These aluminium alloys have a good combination as regards their high corrosion resistance, good formability, medium strength, good machinability and good weldability, and are, therefore, widely used in all kinds of applications (Zhu et al., 2011).

The direct extrusion of aluminium involves shape deformation, heat transfer and a highly complex state of friction, all of which makes this process of metal deformation complicated (He et al., 2012).

The main commercial factors as regards extruded profiles are productivity, cost effectiveness and quality grade, which are directly related to the die performance. There are also other factors, such as the quality

* Corresponding author.
E-mail addresses: juan.llorca@ua.es (J. Llorca-Schenk), JuanRamonRico@ua.es (J.R. Rico-Juan), msanchez@umh.es (M. Sanchez-Lozano).

https://doi.org/10.1016/j.eswa.2023.119808
Received 25 August 2022; Received in revised form 13 January 2023; Accepted 4 March 2023
Available online 9 March 2023

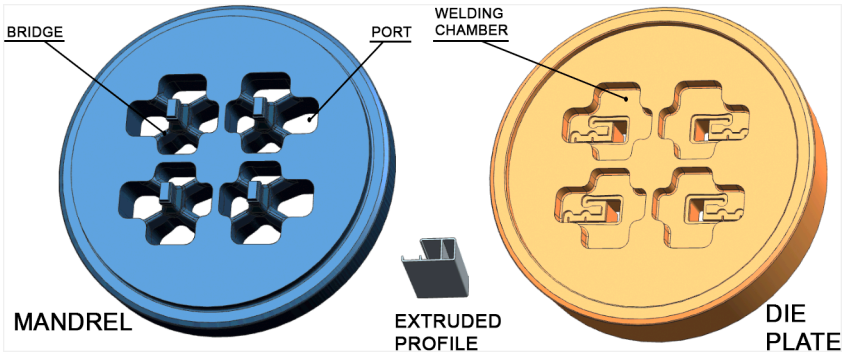

Fig. 1. The components of a typical disassembled porthole die: mandrel and die plate.

of the billet material, the characteristics of the extrusion press, the capabilities of the auxiliary equipment and the final operations, including age hardening, anodising and painting. Perhaps the most critical extrusion component is the die, owing to its high cost, the fact that it requires special materials and processes, its fine tolerances and its high thermo-mechanical fatigue requirements (Arif et al., 2003).

The extrusion of hollow sections is a standard industrial process that is conducted using what are denominated as porthole dies. These consist of two different components: the die plate and the mandrel. The geometry of the die that forms the profile is called bearing and is divided into these two components. In the case of hollow profiles, the die plate shapes the external profile contour (Fig. 1). The internal profile contour is similarly shaped by the outer mandrel contour. In order to allow the aluminium to flow from the front end of the die to the bearing area, a series of holes called ports or portholes are milled into the mandrel. The mandrel areas between the ports or portholes are typically called bridges. The function of the ports is to enable the aluminium to flow into the die, while the function of the bridges is to fix the mandrel core position during the extrusion process. On its way through the die, the aluminium flux is divided by the bridges and forced to flow through the ports. After this, the aluminium flow has to be welded back into the zone of the die plate called welding chamber. Welding takes place in a solid state under suitable temperature and pressure conditions (Ceretti et al., 2009).

The most popular means employed to design extrusion dies is the empirical design approach. Many formulas and design rules have already been introduced and developed. Several authors present empirical solutions for specific topics such as: Bearing length and requirements for automated bearing definition (Miles et al., 1997), or bearing length and die layout design (Lin & Ransing, 2009)….

Another widespread methodology with which to design extrusion dies is based mainly on engineering analogies and on previous similar designs. The finite element method (FEM) can be applied for numerical simulation of the aluminium extrusion process, but the extensive use of such calculations in the extrusion industry is limited owing to the high cost and complexity involved (He et al., 2012).

In the last two decades, many papers have addressed the problem of die design by using FEM simulation as a testing and optimisation tool. Numerical simulation makes it possible to predict the deformations of the parts forming the die and the flow of the aluminium during the process.

The recent review on the use of FEM simulation as a means of assisting the design of extrusion dies by Giarmas and Tzetzis is very noteworthy (Giarmas & Tzetzis, 2022). It contains a large number of studies in which simulation has been applied as a means to solve different design problems in the extrusion die.

Scientific literature contains few recent examples of papers dealing with the fundamentals of porthole die design. There are several publications related to the practical application of FEM simulation in order to improve die design, but they do not usually address the problem of the need to develop an initial design starting point in the optimisation process. It is this shortcoming that the newly developed tool aims to fill.

Some specific papers provide some guidelines on different design points for porthole dies, but these are only basic and general guidelines. Most of these contributions have originated from the biannual International Conference on Extrusion and Benchmark (ICEB). This meeting brings together experts in the aluminium extrusion field with the aim of testing the increased accuracy of numerical simulations for process optimisation and also to discuss the advances as regards knowledge in the field. A different specific die is, therefore, developed for each benchmark: The 2007 edition focused on the design of pockets (Schikorra et al., 2008), and the 2009 edition on the design factors influencing the process of tongue bending in U-shaped profiles (Pietzka et al., 2009). In the 2011 edition, different strategies were used to achieve a balanced flow of aluminium for hollow section extrusion (Selvaggio et al., 2011), in the 2013 edition experimental research was focused on the prediction of the mandrel deflection effects (Selvaggio et al., 2013) and in the 2015 edition the effect of bearing length and bearing shape was investigated (Gamberoni et al., 2015).

Other authors have studied the suitability of using certain special solutions to improve the aluminium flow in multi-cavity porthole dies (Xue et al., 2018). However, none of the available research appears to address the fundamental problem when designing multi-cavity porthole dies: the proper sizing of the feed ports in order to attain a balanced flow. Many studies analyse the flow by employing the FEM in order to propose changes based on the results, but leave aside the need to generate an initial design that is as close as possible to the ideal solution.

The FEM simulation is increasingly being used as a means of aiding the design of extrusion dies, and is a tool for extruders and toolmakers. Commercial software packages have interfaces that make it extremely easy to use, and provide a wide diversity of results: tool stress, tool deflection, profile temperature and differences in extruded profile speed. The possibility of correcting the die design without the need for press trials that is offered by FEM simulation allows reductions in costs. The most notable disadvantage of using numerical simulation is the requirement that simulation experts must carry out model preparation and further analysis. Moreover, the time required for preparation and analysis can be considerable according to the difficulty involved in designing the die. The attractiveness of finite element simulation for extrusion consequently decreases in some cases owing to the extended design times, additional personnel costs and additional software costs (Engelhardt et al., 2019).

Bearing the aforementioned costs and the drawbacks of FEM simulation in mind, the objective of this work is to provide the designer with a machine learning (ML) based tool in order to assist in the sizing of the ports of porthole dies. The purpose is to assist in the definition of an optimal initial design of highly complex porthole dies with the aim of minimising the modifications required after FEM simulation. This avoids having to design the dies depending only on the designer's experience and, in the best case, on the final adjustments introduced thanks to the

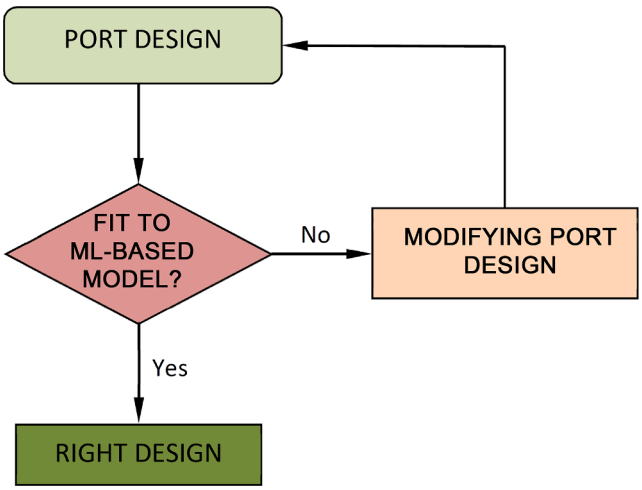

Fig. 2. Design methodology diagram.

process simulation.

The main source of severe flow troubles during extrusion in porthole dies is the wrong dimensioning of the ports (area, position…), which can lead to a large deviation of the profile or large lateral mandrel deflections and modifications to the profile thicknesses.

As mentioned previously, many documents provide recommendations and guidelines for die design or specific formulas with which to define some specific detail in porthole dies. But none of them offers an accurate and structured formulation to assist in the sizing and design of porthole dies.

It is possible to state that, in order to reach an effective design of porthole die, it is essential to guarantee:

- The mechanical strength of all its components.
- A uniform outlet velocity in the extruded profile section during the whole forming process.

On the one hand, resistance calculations allow optimum mechanical properties to be ensured.

On the other, the main design variables required in order to attain a uniform outlet velocity in the extruded profile are: the balanced definition of the geometry of the ports so as to ensure a uniform velocity of the aluminium in the die welding chamber, the optimal definition of the welding chamber (Donati & Tomesani, 2004) and the optimised sizing of the bearings according to the profile thickness and its position in the die.

These are the main factors but it should be noted that there are some other secondary factors and decisions to be made during the design process that also influence the flow balance: profile layout, shape of the bridges….

For the vast majority of these design factors, there are references that provide guidelines to facilitate the optimal choice. Among all of them, the balanced dimensioning of ports is the critical aspect that is least supported by clear guidelines.

Defining balanced ports in a porthole die is not so easy because during the extrusion process the velocity of the aluminium inside the billet is not uniform. The velocity and pressure distribution of the aluminium at the inlet face of the extrusion die are both concentric owing to the friction between the container wall and the billet (Mori et al., 2002). This results in the maximum velocity being in the centre of the die and the minimum velocity in the outer area.

Furthermore, it should be noted that ML is an area of Artificial Intelligence and a discipline that is being used to an increasing extent in more and more areas, including industry and engineering. The basic reason why ML models have barely been applied in data analysis to date is because their interpretation is complex, and they are often colloquially called black boxes (Koh & Liang, 2017).

Nevertheless, recent advances in what is known as eXplainable Artificial Intelligence (XAI) allow useful and understandable

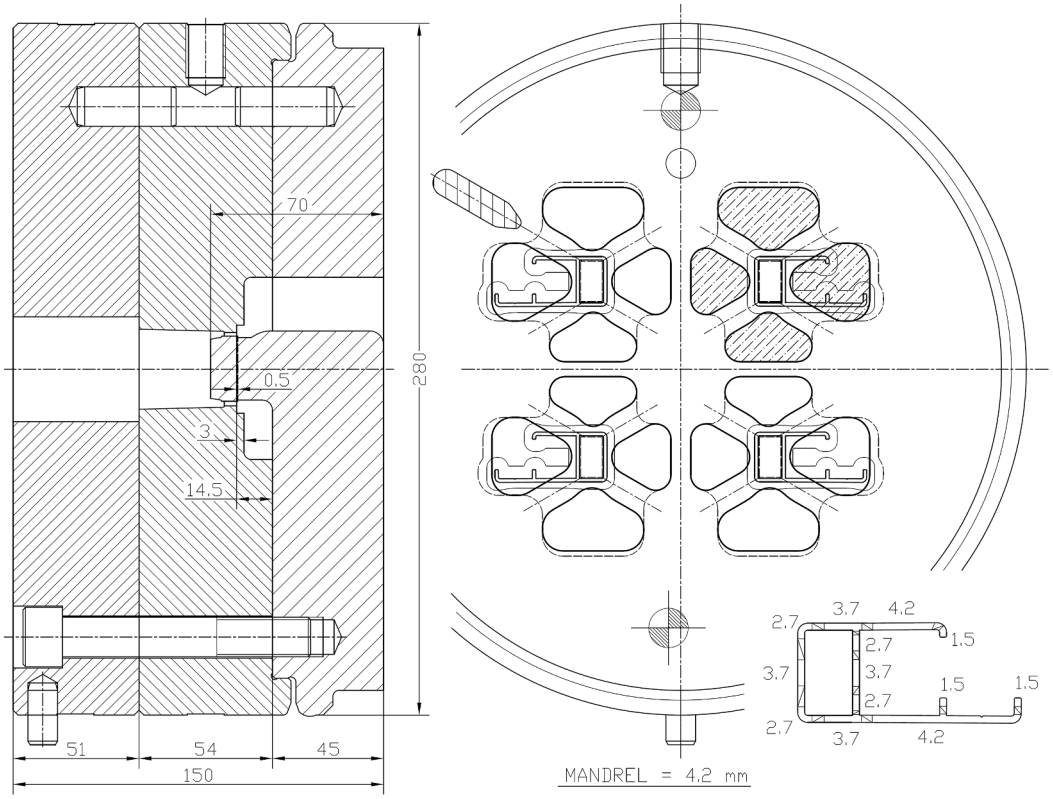

Fig. 3. Example of a four-cavity porthole die with four ports per cavity (port geometries shown hatched in the upper right cavity).

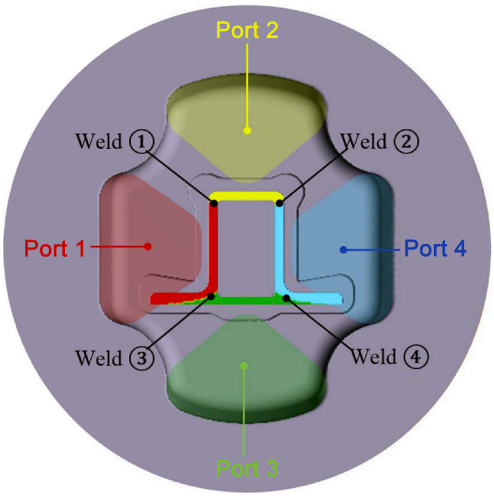

Fig. 4. Portions of the extruded profile owing to material distribution in the ports. Source: (Yu et al., 2019).

information to be extracted from predictive models (Barredo Arrieta et al., 2020). More specifically, techniques based on post-hoc analysis enable a unified approach to explain the prediction performed by any ML model. SHAP (SHapley Additive exPlanations) is an example of a tool of this nature, which is based on game theory and is able to extract information concerning the importance of variables at both global and local levels (S. Lundberg, 2019).

ML is currently being applied in different areas. Some examples are its application to: industry in general in order to deal with new challenges (Dalzochio et al., 2020), logistics (Liu, 2021), finance (Chen & Chang, 2021), and specifically the impact of FinTech patents and energy (Narciso & Martins, 2020). There are even different examples of the application of Artificial Intelligence in the extrusion industry. These applications focus on the development of models for the appropriate choice of the optimal process parameters (Lucignano et al., 2010) and for the choice of the optimal layout for a die (Yan & Xia, 2006).

With regard to the application of ML to tool engineering, the objective of the new ML-based model is to facilitate the development of an initial design that is as close as possible to the optimal design in a way that eliminates or minimises the need for FEM simulation in order to ensure a perfectly balanced aluminium flow in the die during extrusion.

There is a recent precedent: a similar tool based on linear regression (Llorca-Schenk et al., 2021). This is a design tool grounded in engineering by analogy. But it does not follow the traditional methodology in which the analogy focuses on a single design. In this case, the model collects the experience and know-how accumulated in many optimal designs and can, therefore, help to create a new design by analogy on the basis of this whole group of reference designs.

One of the drawbacks of the aforementioned model is that it is based exclusively on linear predictions, when most real problems usually contain variables with non-linear relationships. In the present paper, a step further will be taken and this tool will be improved by means of a new proposal based on ML algorithms that extract both linear and non-linear relationships, thus making more accurate predictions and generating die designs that are closer to the designs of the reference set.

2. Materials and methods

2.1. Method overview

The overall purpose of this research is to provide a tool with which to assist die designers to obtain port geometries for porthole dies that achieve a balanced flow of aluminium during extrusion.

It is first necessary to decide which criterion to use in order to consider that the ports of a porthole die are “balanced”.

The most widespread design criterion is that of equalising the concentric velocity differences in the aluminium billet by means of the proper positioning and sizing of the porthole die ports (Mori et al., 2002). The aluminium flow must, therefore, be able to equalise its velocities and pressures in all the ports, from its entry at the front end of the die through the ports to its arrival in the welding chamber of the die. After achieving a balanced design of all ports using this criterion, the definition of the bearings in the profile geometry is simple because it depends mainly on the thickness of the profile.

The trouble of the port sizing of porthole dies mainly appears in multi-cavity dies, since several ports are located at very different distances from the centre of the die. The concentric velocity distribution at the front end of the die means that the die ports must be sized in order for their area to perimeter ratio to depend on their distance to the centre of the die.

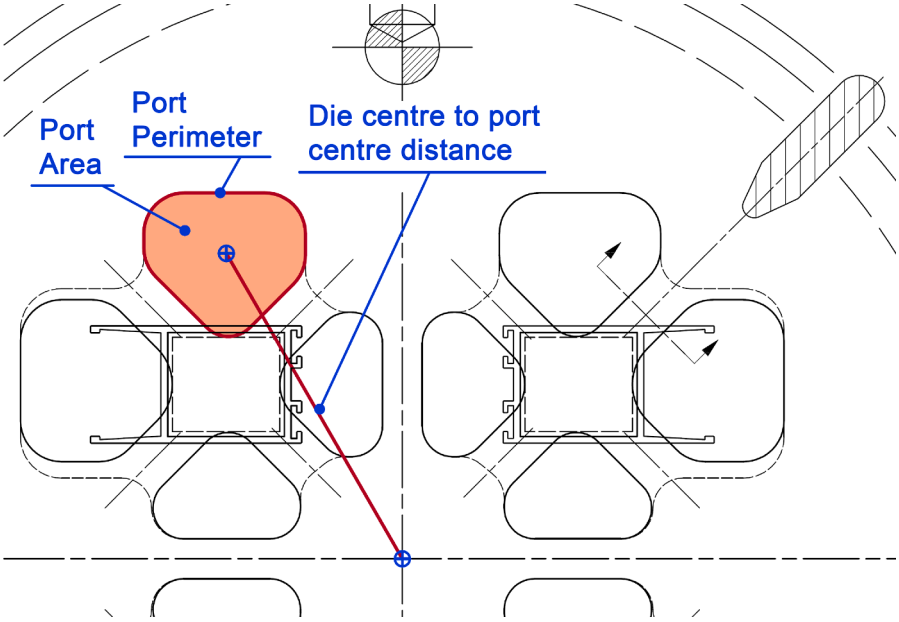

Fig. 5. Variables that geometrically define the port of a porthole die.

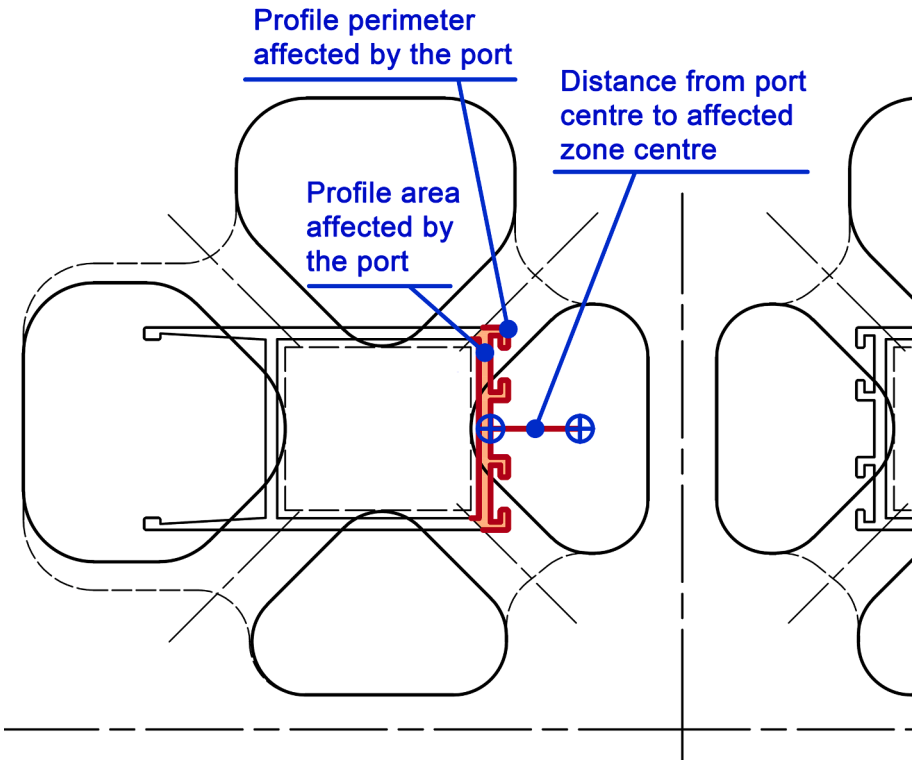

Fig. 6. Variables employed in order to account for the influence of the portion of the extruded profile affected by each port.

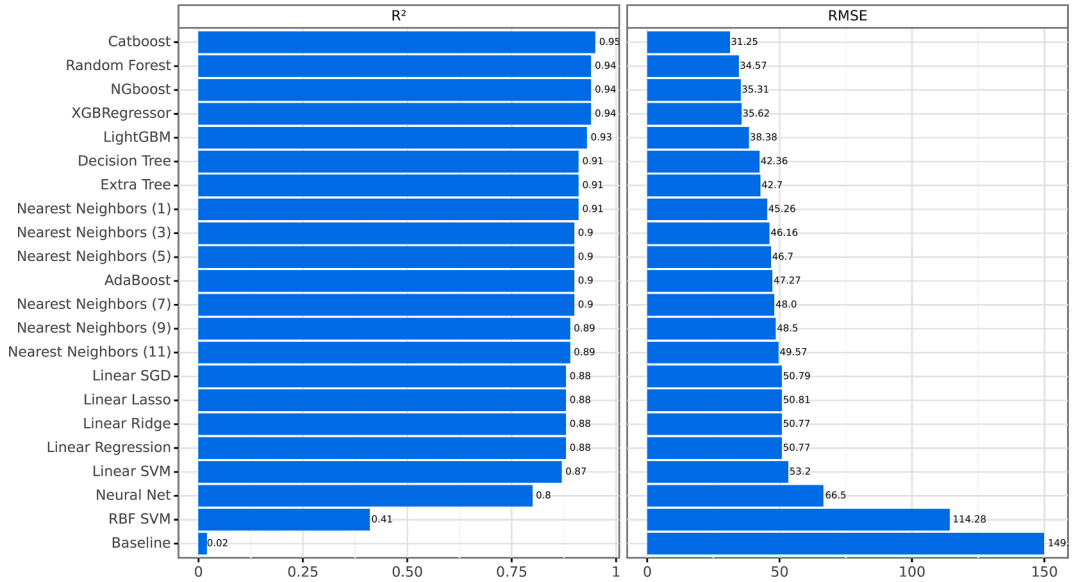

Fig. 7. Average results of 10-CV of R^2 and RMSE sorted in ascending order by the R^2. The higher R^2 value is better, while in the case of RMSE, the lower value is better.

Experienced designers consider that it is intuitively plausible to find some kind of balancing function linking correctly some important geometrical variables of the ports (area, perimeter and distance to the centre of the die) and the geometrical variables of the profile zones influenced by the related port.

It would, however, appear to be very complex to create an automatic application that automatically generates balanced port geometries from scratch. The port geometry depends on many limiting factors and has to be adjusted to the profile geometry. The alternative solution chosen could be the definition of a tool with which to validate new port geometries, thus guaranteeing a balanced port design.

In order to achieve this objective, an advanced analysis based on machine learning and explainability techniques (ML-XAI) has been chosen that allows a better approximation (it is not necessary for the data to follow a normal distribution, in addition to which non-linear relationships between them are estimated). This will make it possible to identify the impact of the predictor variables on the prediction, the dependencies between them and the prediction of samples to act accordingly. The different analyses have been applied to the same dataset in order to determine which is the most appropriate as regards

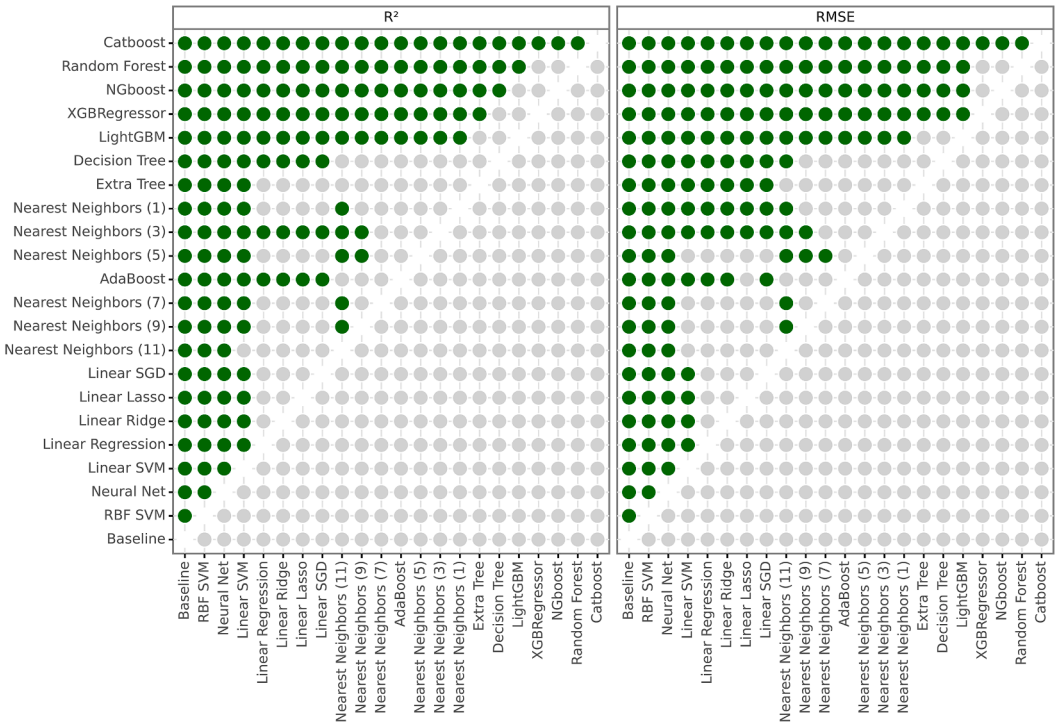

Fig. 8. Comparison of significance with the Wilcoxon test between pairs of algorithms based on the results obtained in the 10-CV with the R^2 and RMSE metrics. Each green circle indicates that the row algorithm is significantly better than the column algorithm at 95%. A higher number of green circles in a row indicates a better algorithm. (For interpretation of the references to colour in this figure legend, the reader is referred to the web version of this article.)

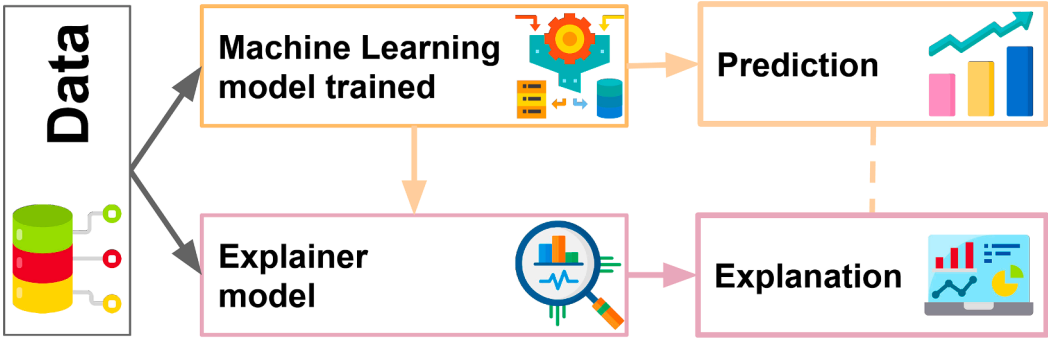

Fig. 9. General diagram of machine learning models' post-hoc explainability.

fitting the data to the new model.

A question now arises: How can a model relating the variables, defining the geometry of balanced ports in a die, assist designers to attain an optimal design?

In order to use the new model, after developing an initial port design, the designer must check whether the ports designed fit the ML-based model. If the ports created do not fit the model according to a previously defined acceptance criterion, the port design must be amended in the correct direction in order to reach an equilibrium situation. These amendments must be performed repeatedly until a port configuration that fits the ML-based model according to the defined acceptance criterion is achieved (Fig. 2).

Owing to the huge variety of existing die designs, following some experiments with the previous model based on linear regressions, it was concluded that the best way in which to attain suitable results is to group the designs of dies by several typologies. Since the aim is obtaining a balanced port design, the typologies have been defined according to the number of die cavities and the number of ports per cavity (Llorca-Schenk et al., 2021).

This research focuses on the most common and widespread four-cavity porthole die designs for mid-sized profiles in all applications: four-cavity porthole dies with four independent ports per cavity (Fig. 3).

It is now necessary to ask the following: what methodology has been used to develop this predictive model relating the geometric variables involved in a balanced port design?

The approach is based on obtaining a predictive model chosen from a series of probes with different algorithms belonging to several machine learning (ML) families. Moreover, the application of explainability techniques provides an insight into different aspects of the model, such as the importance of the predictors, linearity or non-linearity relationships, or interactions and variations in the prediction according to the characteristics of the sample.

The geometric variables associated with 596 different ports have been analysed on the basis of 88 proven efficacy four-cavity, four-port-per-cavity porthole die designs. These are dies that have been used in presses with a container diameter of 178 mm and 16000MN force or with a container diameter of 203 mm and 22000MN force, all of which use 6063 aluminium alloy as a billet material and are made of H-13 hot

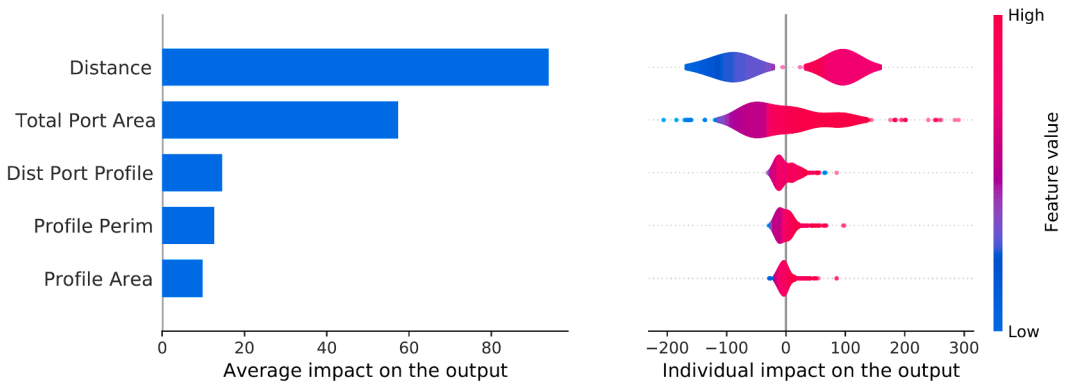

Fig. 10. Importance of predictors and their impact on the outcome variable (Port Area). Left: general importance. Right: positive or negative impact broken down by sample. Magenta indicates higher values and blue lower values. (For interpretation of the references to colour in this figure legend, the reader is referred to the web version of this article.)

work steel. These two typologies of extrusion presses have extremely close flow behaviour because their maximum pressure is practically the same. Numerous extruders have one press of each of these typologies simultaneously, and often use dies initially designed for the 7″ press on the 8″ press with equivalent flow balance results.

The proven efficiency of all these dies is based on the fact that they are all first-trial dies designed and produced by HAEP, S.A. (Hydro Aluminium Extrusion Portugal). After the first extrusion test, the behaviour of the die was optimal and the profile samples were approved according to the criteria and tolerances established by EN-12020-2 standard (according to the feedback after the extrusion test).

Given the methodology and the material data used for the development conducted, the model will be suitable for the working temperature range of the 6xxx series aluminium alloys during extrusion: 400–550 °C.

3. Dataset

The initial stage when defining the model for this new design assistance tool was to determine which variables would be fundamental for the geometrical definition of the ports in a porthole die. This large number of defining geometrical properties was first compiled for each port:

1. Port area.
2. Port perimeter.
3. Distance from die centre to port centre (distance from die centre to areas' centre of areas of port).
4. Area of the extruded profile portion affected by the related port (see Fig. 4 and Note 1).
5. Perimeter of the extruded profile portion affected by the related port (see Fig. 4 and Note 1).
6. Distance from the centre of areas of port to centre of areas of the extruded profile zone affected by the related port (see Fig. 4 and Note 1).
7. Total perimeter of the full port set of the die
8. Total area of the full port set of the die

Note 1: The extruded profile can be divided into several portions, and each of these portions is formed by the aluminium flowing through each port. These profile portions are bounded by the welding lines of the bridges (Yu et al., 2019).

Each of these variables is briefly explained below with the support of several figures. The variables that geometrically define the port design of a porthole die are (Fig. 5):

- The *Port Area* variable, which determines the amount of aluminium entering into that area of the die.
- The *Port Perimeter* variable, which determines the friction that the die presents to the flux of aluminium through the port.
- The *Distance from die centre to port centre* variable, which determines the velocity of the aluminium in the inlet face of the port. The precise location of the port is not important owing to the concentric distribution of velocities in the billet, but its distance to the centre is. Ports of identical area and whose position is symmetrical with respect to the centre of the die therefore behave in the same way during the extrusion process.

The following variables have been considered to account for the influence of the portion of the extruded profile affected by each port (Fig. 6):

- The *area of the extruded profile portion affected by the corresponding port* determines how easily the aluminium can flow through that zone of the die. Therefore, it also conditions the amount of aluminium that should feed the port in order to ensure a well-balanced flow.
- The *perimeter of the extruded profile portion affected by the corresponding port* determines the profile restraining capacity for the free aluminium flow in that zone of the die. Therefore, it also conditions the amount of aluminium that will feed the port in order to achieve a well-balanced flow.
- The *distance between the port centre and the centre of the areas of the extruded profile zone affected by the port* quantifies how directly the profile is exposed to the flux of the aluminium in the port.

Two additional geometric variables corresponding to the full port set are also included because, based on experience, the same die may be balanced with larger or smaller ports. These global variables, therefore, make it possible to integrate the issue of whether the design will use major or minor ports into the model. These aggregate variables are:

- The *total area of the full port set*, which determines the overall amount of aluminium that will flow into the die.
- The *total perimeter of the full port set*, which determines the overall friction that the die presents to the flow of the aluminium.

In order to facilitate data collection, a C# application of our own development was used to capture the data of the 2D CAD designs of the dies. This application greatly speeds up the task by facilitating the selection of geometries and orderly writing the geometry data for all variables. The units used in all data collection were millimetres and square millimetres.

Port Area was chosen as the dependent variable because it is commonly used as the characteristic identifying variable for each port

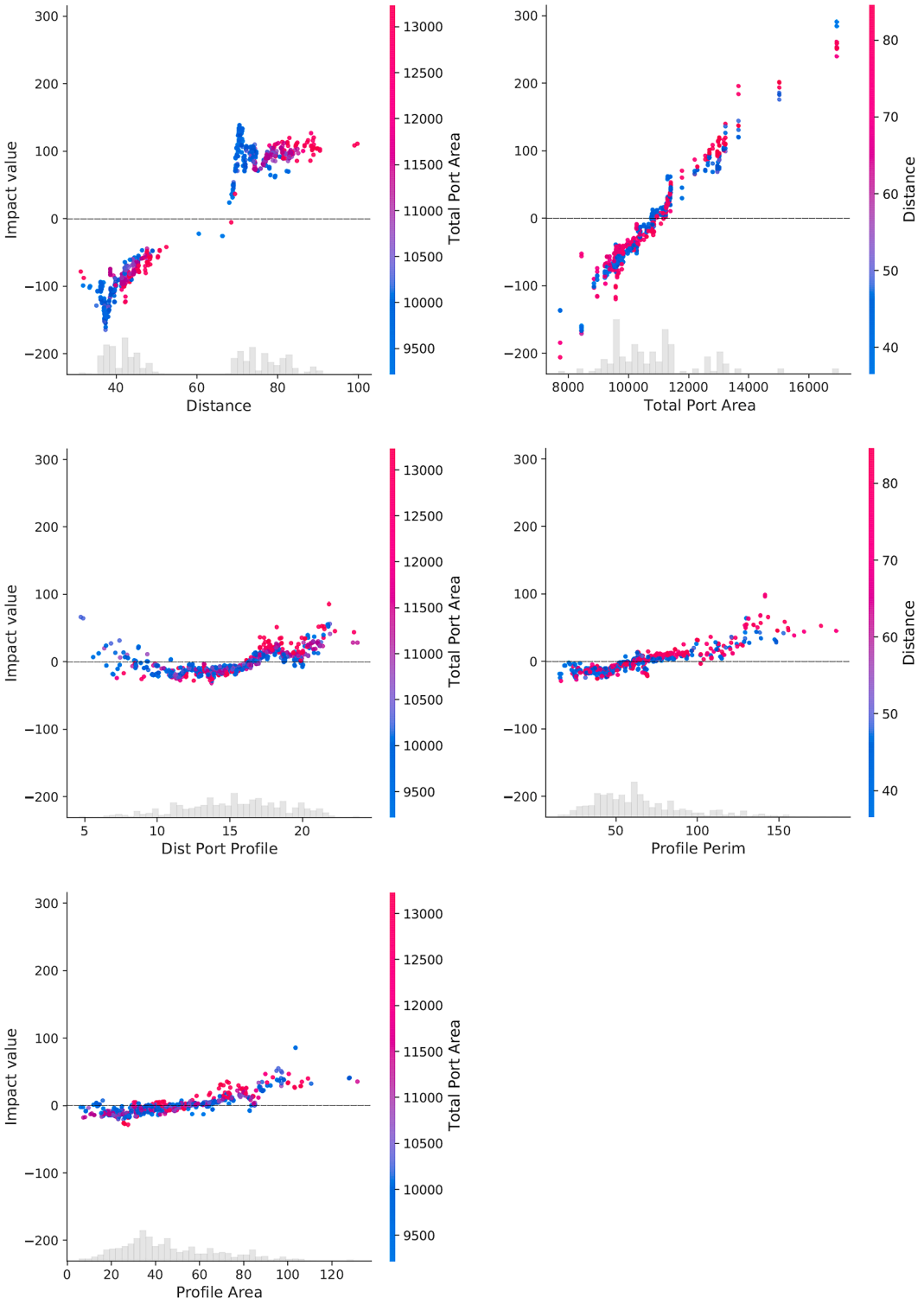

Fig. 11. Scatter plot per predictor. Each plot shows the individual impact of each sample value on the outcome, and red/blue show the relation with a close predictor interaction. The histogram of the sample values is shown in grey at the bottom of each graph. (For interpretation of the references to colour in this figure legend, the reader is referred to the web version of this article.)

Table 1
Example of a correctly constructed die.

Distance (mm)	Profile Area (mm^2)	Profile Perimeter (mm)	Total Port Area (mm^2)	Distance Port Profile (mm)
84.2	74.4	116.2	11184.6	10.3

Port Area: True value 813.7 Predicted: 817.9 RMSE: 4.2.

Table 2
Example of die with recommendations for revision.

Distance (mm)	Profile Area (mm^2)	Profile Perimeter (mm)	Total Port Area (mm^2)	Distance Port Profile (mm)
42.2	32.4	56.0	9577.4	12.9

Port Area: True value 603.1 Predicted: 562.4 RMSE: 40.7.

during the design process (changes and adjustments for flow balancing in ports are usually based on port area modifications).

As occurred with the previous linear regression-based tool, the *Port Perimeter* and *Total perimeter* have been discarded as independent variables. In the case of the linear regression-based tool, this discard was justified on the grounds that there was a high partial correlation between the area and these variables. And this correlation was not owing to phenomena inherent to the extrusion process but rather to a simple geometric linkage (Llorca-Schenk et al., 2021).

Bearing these considerations and the aforementioned discards in mind, the set of independent variables used in the analysis is formed of the following group:

1. *Distance*: distance between the die centre and the port centre.
2. *Profile Area*: area of the extruded profile portion affected by related port.
3. *Profile Perimeter*: perimeter of the extruded profile portion affected by related port.
4. *Distance Port Profile*: distance between the centre of areas of port and the centre of areas of the extruded profile zone affected by related port.
5. *Total Port Area*: total area of the full port set of the die.

3.1. Explainable machine learning

Several families of algorithms have been tested to obtain the best of the models to make good predictions, and thus explain more precisely the relationship between independent and dependent variables. To explore different ML-based approaches, algorithms belonging to different families have been chosen such as those based on neighbourhood, support vector machines, linear regression, decision trees and neural networks, in order to find that which obtains the best results for the studied dataset.

The chosen algorithms are presented below together with a brief description of them:

- Baseline: As a starting model, the average value of the outcome variable is defined as a prediction.
- Linear Regression: This regressor is based on the calculation of multiple linear coefficients of the predictor variables and an intercept value with a least squares approach. In addition, other variants have been used such as Ridge (Hoerl & Kennard, 1970), LASSO (Tibshirani, 1996) and SGD (Sharma, 2018) in which the term to be optimised varies.
- Decision tree (Breiman et al., 1984): This model is based on predicting values by applying hierarchically structured rules. The rule tree itself is constructed from the training set, and uses a single feature in each rule.
- Random Forest (Breiman, 2001): Several decision trees are built to combine all the predictions into one. This combination leads to a more robust behaviour.
- AdaBoost (Adaptive Boosting) (Freund & Schapire, 1997): This algorithm uses several linear regressors. The final decision for a new sample is made based on the confidence learned for each regressor set in the training phase.
- XGBoost (Chen & Guestrin, 2016), LightGBM (Ke et al., 2017) and CatBoost (Dorogush et al., 2018): These algorithms are based on the application of booting to decision trees, in which optimisation is conducted by means of derived cost functions and the lowering of gradients as in neural networks. Each algorithm applies these types of optimisations in different ways and has performed well in open challenges.
- Support vector machines (Cortes & Vapnik, 1995): These algorithms are based on two phases. In the first phase, the original data space is mapped onto another space, usually of a higher dimension. While the second phase tries to locate a linear hyperplane of separation in the resulting space.
- Neural Network (Multilayer Perceptron) (Hinton, 1989): This type of neural network is well established and all its layers are completely connected to each other.
- Nearest Neighbours (Cover & Hart, 1967): The prediction value is calculated on the basis of the closest k (parameter) samples of the training set. The concluding prediction is an interpolation based on the proximity of those neighbours using the Euclidean distance. In this study, the k parameter was set at 1, 3, 5, 7, 9 and 11.

4. Results

4.1. Experimentation

The validation strategy used for comparing the predictive ability of the models when applied to new observations was on the basis of the comparison of K-Fold Cross-Validation estimators, with the value k = 10. The metrics employed for the evaluation of the models are those commonly used for this purpose. They are on the basis of measuring of the explanatory degree of the model, the R^2 score (1), and the prediction

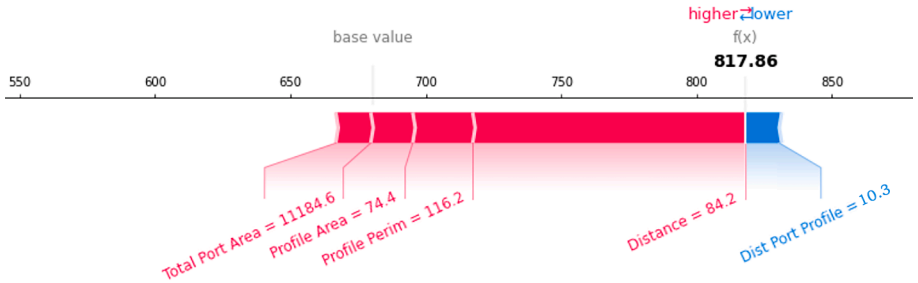

Fig. 12. Contributions of each variable to the predicted *Port Area* value, for a port case with a low RMSE.

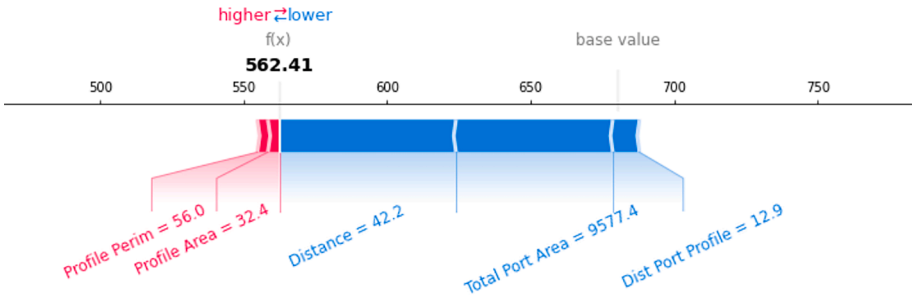

Fig. 13. Contributions of each variable to the predicted Port Area value, for a port case with a high RMSE, thus suggesting a revision of the design.

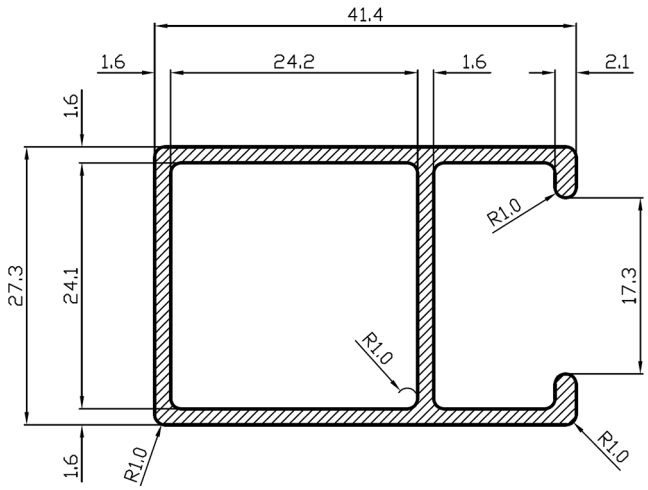

Fig. 14. Profile of the application example.

errors as the root mean squared error (RMSE) (2). In these equations, the variables y and ŷ are the true and predicted values, respectively.

$$R^2(y,\hat{y}) = 1 - \frac{\sum_i^n (y_i - \hat{y}_i)^2}{\sum_i^n (y_i - \bar{y}_i)^2} \tag{1}$$

$$RMSE(y,\hat{y}) = \sqrt{\frac{1}{n}\sum_i^n (y_i - \hat{y}_i)^2} \tag{2}$$

Besides considering the previous results (Fig. 7), which are averages of the cross validation (CV), it is convenient to contrast them in order to discover whether or not the difference between the algorithms is significant. The Wilcoxon paired test (Wilcoxon, 1945) with the most commonly used confidence value of 95% is employed for this purpose.

A comparison between the statistical significance of algorithm pairs according to the R^2 and RMSE metrics is shown in Fig. 8. The following conclusions can be drawn:

1. Baseline, linear regressions, SVM and neural networks attain the worst results
2. Nearest neighbours and tree algorithms obtain average results.
3. The algorithms based on the generation of multiple decision trees together with the boosting technique achieve the best results, with CatBoost being significantly better than the rest.

4.2. Machine learning explainability model

The best results are generally achieved with complex models commonly referred to as 'black boxes'. And there are two approaches with which to attempt to provide consistent explanations for their predictions in a coherent manner once trained with data (post-hoc):

The first post-hoc explainability approach is on the basis of carrying out permutations on the values of each predictor (individual input variable) and directly comparing the variability as regards its predictions (Breiman, 2001). This makes it possible to estimate the importance of the predictors of an already trained model.

The second approach, which is more accurate than the first, is based on the construction of a new linear model with which to explain the complex model already trained. The calculation of Shapley values provides a solution that equitably distributes an interaction between independent and dependent variables (Roth, 1988). This approach is often used in situations in which features contribute unevenly. In essence, a Shapley value reflects the average marginal contribution expected from one variable after considering all possible combinations with other variables. This method also ensures local accuracy, missingness and consistency. This approach uses a local linear approximation to explain the behaviour of the ML model (Fig. 9), although most of models use internally non-linear mechanisms to relate the input variables to the output variable (target).

Recent advances related to this approach are explained by Lundberg and Lee (Lundberg & Lee, 2017). This approach allows a unified approach to explain the predictions made by any self-learning model already trained. An example of such a post-hoc approach is the SHapley Additive exPlanations (SHAP) tool, which is based on game theory and allows the extraction of both local and global explanations (Lundberg, 2019).

This explainability of the machine learning model can be of great interest when attempting to approximate the values of a design that is outside the range defined as correct. In these cases, the procedure would be to define a new design with new geometric characteristics. These characteristics can be defined properly and as quickly as possible by studying the individual contributions of each of the variables, particularly those variables that are most easily modifiable in the port design: centre distances and areas.

4.3. Importance of the model's features

The features of the model and their importance depend directly on the data used and the model itself. In this case, the Catboost algorithm is used, owing to the results given in Section 3.1.

The Shapley values are calculated separately in the trained model and their accumulated absolute values determine their importance. Fig. 10 shows the model's predictors in order of importance.

As might be expected, given the results obtained by predecessor models based on linear regression (Llorca-Schenk et al., 2021), the predictors *Distance* and *Total Port Area* clearly have the greatest impact on the output variable.

The *Distance* directly conditions the output variable, *Port Area*, because in order to achieve a design with a balanced flow of aluminium, it is observed that:

- Owing to the concentric distribution of velocities and pressures (Mori et al., 2002), the greater the distance between a point and the

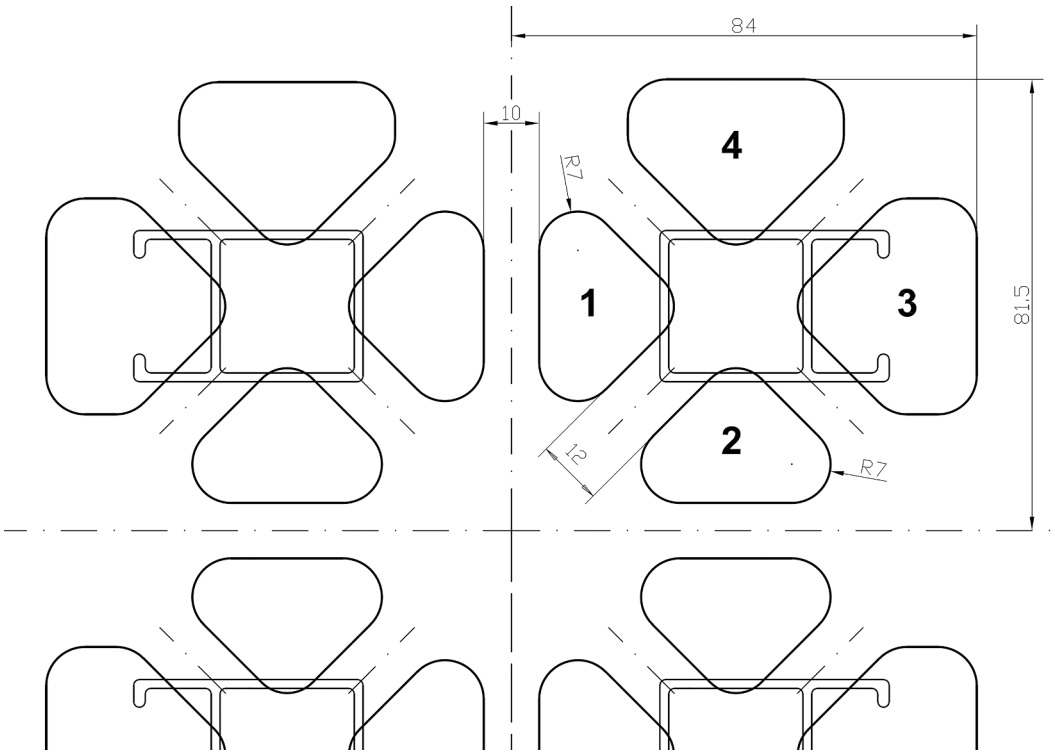

Fig. 15. Initial four-cavity design developed for example die.

Table 3
Value of the variables for the initial design of the example die.

Port	Port Area (mm2)	Distance (mm)	Profile Area (mm^2)	Profile Perimeter (mm)	Total Port Area (mm^2)	Distance Port Profile (mm)
1	599.59	43.17	40.84	55.49	12031.63	12.68
2	599.59	43.17	40.90	55.88	12031.63	12.72
3	953.12	81.46	99.06	121.75	12031.63	11.93
4	855.61	80.32	40.90	55.88	12031.63	15.94

die centre, the lower the velocity and pressure at that point of the aluminium billet before it enters the die.
- In order to achieve aluminium-flow balance, therefore: the greater the distance from die centre, the greater the port area required.

Furthermore, the *Total Port Area* is also fundamental because it conditions the overall size of the ports in a die. A balanced die can have a design of ports of a larger or smaller area, but all of them must have an adequate ratio between their sizes. This variable, therefore, in some respects serves to introduce the condition of the global size of all the ports of the die.

The three variables with the lowest impact reflect different aspects of the influence of the profile on the port. As shown in Section 2.2, each of the variables provides different nuances of the influence of profile geometry as regards achieving a port with a balanced flow of aluminium.

Fig. 11 shows the individual impact of each sample value on the outcome (*Port Area*). Moreover, red/blue show the relation with close predictor interaction.

By analysing the point distributions of these scatter plots, it is possible to draw some conclusions regarding the different relationships between the output variable and each of the predictors. Moreover, in some cases the colour coding also makes it possible to conclude some relationships between the predictors.

The relationships and conclusions to be drawn are the following:

1. The behaviour of the *Distance* predictor is, in general terms, quite close to being linear. In this case, if the colour code is analysed, it shows different behaviour for the smaller *Total Port Area* values and the larger ones: the smaller values appear to have a steeper slope on the line they describe, while the larger *Total Port Area* values describe a line whose slope is clearly less steep.
2. The subfigures *Total Port Area* and *Profile Perimeter* show that the behaviour of these predictors is practically linear.
3. The subfigure *Profile Area* indicates a certain non-linearity of this variable. However, it should be noted that only large area values (above 60 mm^2) have a considerable impact, and that the impact is close to zero for the rest of the values.
4. Finally, the subfigure *Distance Port Profile* shows clearly a non-linear relationship with the outcome.

As expected, given the R^2 results of the different algorithms discussed in Section 3.1, the behaviour of some of the predictors is somewhat more complex than linearity. This is why the more complex algorithms clearly achieve a better coverage of the variability of the data than Linear Regression.

4.4. Methodology used in order to apply the model as a design aid tool

The process shown below is employed in order to use this model as a design aid:

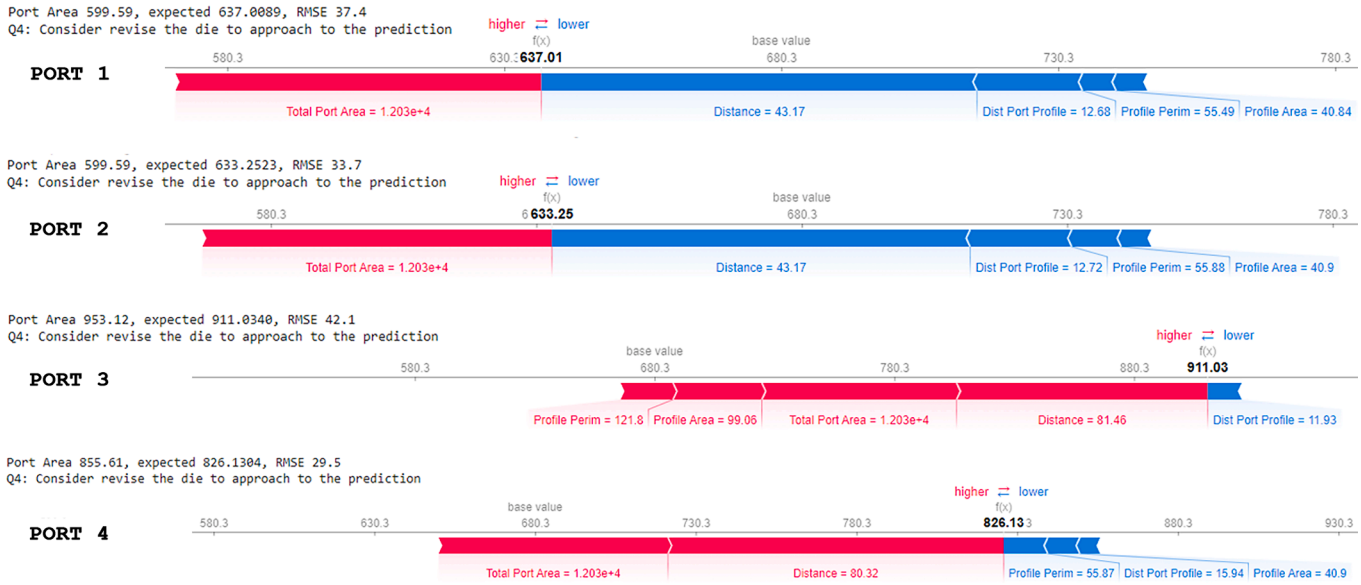

Fig. 16. Predictions obtained by the ML-based model for the ports of the initial design, with the contributions from each of the variables.

Table 4
Analysis and recommendations provided by the ML-based model for the initial design ports.

Port	Port Area (mm2)	Expected Port Area (mm^2)	RMSE (mm^2)	RMSE quantile	Model recommendation
1	599.59	637.01	37.4	Q4	Upward revision
2	599.59	633.25	33.7	Q4	Upward revision
3	953.12	911.03	42.1	Q4	Downward revision
4	855.61	826.13	29.5	Q4	Downward revision

1. A first set of port design is made for a die based on the designer's previous knowledge and experience.
2. The values of the variables for each port are entered into the created Catboost model. The model is available for testing at the following link:
   https://colab.research.google.com/drive/1lM2-ZGC6tB4MxnT6AuxMzxyb1PX4AkYa?usp=sharing
3. The *Port Area* value of the design is compared with the *Port Area* value predicted by the model as correct. According to this comparison:
   - If the RMSE (root-mean-square error) value is between the quantiles Q1 and Q2, the *Port Area* designed is considered to be perfectly adjusted to the predicted model and the design is, therefore, considered to be completely correct.
   - If the RMSE value is in quantile Q3, the *Port Area* is considered to be moderately well fitted to the model. A possible modification with which to improve the design could be considered.
   - If the RMSE value is higher than Q3, it is clearly necessary to revise the design in order to improve it.
   - The RSME quantile cut-off values obtained by the Castboost model are: Q1 $\leq$ 2.75, Q2 $\leq$ 5.66, Q3 $\leq$ 9.95, Q4 $\leq$ 47.64
4. Any revisions of these initial designs must rely on the help provided by the explainability of the model. The value recommended by the model can be better approximated by studying the variables that explain the value obtained.

Below are 2 example sets of port design values. One of them fits the model correctly (Table 1) (Fig. 12), while the other should be revised (Table 2) (Fig. 13). It is important to note that the explainability of the graphs provides information about the contribution of each of the variables from a mean or base value (according to the length of the segment) and the direction, positive or negative, of the contribution of each of the variables from a base value (according to the colour of the segment). As indicated previously, observing the weight and direction of the contributions of the different variables that explain the value obtained shown in the graphs makes it possible to choose the best way in which to approximate the value recommended by the model.

5. Application example

5.1. ML-based model application

The different steps of the process of applying the new ML-based model to an example case are detailed below:

1. First, starting from the geometry of the profile for which a die production is desired, a design of the set of ports is created according to the design criteria imposed by the geometry of the profile and the designer's experience (the ML-based model is not involved in this stage of the process).
2. The geometric data of the newly designed set of ports is collected and entered into the ML-based model.
3. The port area value that the ML-based model indicates as correct is compared to the initial design area value, for each of the designed ports.
4. Depending on the quantile in which the RMSE is found, a decision is made regarding the suitability of the port design following the criterion provided in section 3.4.
5. If the RMSE is within the Q3 quantile, a revision of the design is appropriate, and if it is above the Q3 quantile, a revision of the design is essential.
6. In order to make these modifications, it is advisable to rely on the explainability of the model to help identify the most appropriate direction and way in which to make the changes that will allow us to approach the value of the variables that best fit the model.
7. After making the appropriate changes, the ML-based model is re-evaluated for all ports (the model value changes for the remaining ports if any port changes, because the Total Area variable participates in the model). If any port still has RMSE values outside the desired range, steps 5 to 7 must be repeated until all ports are within the required range (Fig. 2).

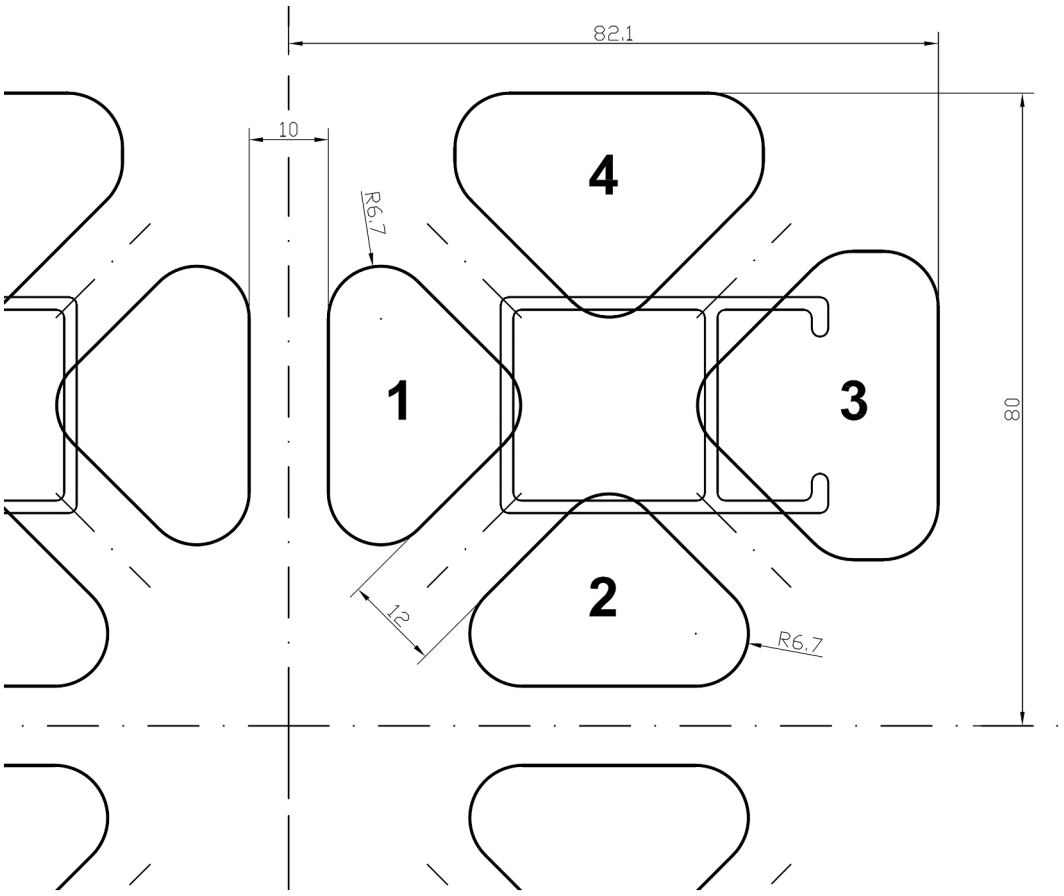

Fig. 17. Improved four-cavity design for the example based on the ML-based model indications.

Table 5
Value of the variables for the improved design of the example die.

Port	Port Area (mm2)	Distance (mm)	Profile Area (mm^2)	Profile Perimeter (mm)	Total Port Area (mm^2)	Distance Port Profile (mm)
1	610.16	43.2	40.84	55.49	11585.76	12.83
2	610.16	43.2	40.90	55.88	11585.76	12.87
3	879	80.59	99.06	121.75	11585.76	10.98
4	797.12	79.63	40.90	55.88	11585.76	15.44

Fig. 18. Predictions obtained by the ML-based model for the ports in the improved design, with contributions from each of the variables.

Table 6
Analysis and recommendations provided by the ML-based model for the improved design of ports.

Port	Port Area (mm2)	Expected Port Area (mm^2)	RMSE (mm^2)	RMSE quantile	Model recommendation
1	610.16	610.90	0.7	Q1	Properly fitted
2	610.16	608.00	2.2	Q1	Properly fitted
3	879.00	878.14	0.9	Q1	Properly fitted
4	797.12	795.86	1.3	Q1	Properly fitted

When adjustments to the geometry are necessary in order to correctly fit the values to the ML-based model, one of the 2 most easily controlled geometric variables is usually used: *Port Area* or *Distance*. A modification to the area of the port is, in general, usually easier because it is difficult to modify the position of the profile due to other design conditions. It is, therefore, possible to state that the most effective method by which to modify the geometrical characteristics of a port is by changing the port zone furthest from the profile in order to modify its area.

Fig. 14 shows the profile for which a four-cavity, four-port-per-cavity design is desired for a press with a 203 mm container and a force of 22000MN.

The designer must start by using this profile data to start the design of the die. The example focuses on the design of the mandrel ports, for which the ML-based model has been developed, although the die design includes other steps.

The designer must initially place the cavities of the profile with respect to the die centre with the constraint of the bolster support. For the layout, the most common choice for this type of profile is the symmetrical arrangement and orientation of the profile with support on the face, which provides greater stability (Saha, 2000).

A first attempt is then made to design the ports, considering the location established for the profile and the need to leave a minimum bridge width of 10–13 mm (minimal distance between ports).

With these design criteria, the designer performs the first design attempt. It is a vertically and horizontally symmetric design, with 12 mm bridges and central walls of 10 mm (Fig. 15).

For these initial geometries, the value of the variables involved in the ML-based model are given in Table 3. These values have been fed into the model in order to obtain the results shown in Fig. 16 and Table 4. These show the predictions obtained by the ML-based model, the RMSE between the value of the initial design and that predicted by the model, and the quantile to which this RMSE corresponds.

The ports numbered 1 and 2, therefore, have to be increased in area in an attempt to fit the model properly. Furthermore, the ports numbered 3 and 4 have to be reduced in area in an attempt to fit the model adequately. Since some other variables are linked to changes in the *Port Area*, it is extremely difficult to estimate the exact extent to which the area of the ports should be adjusted, and an iterative approximation must, therefore, be made in the direction indicated by the model.

At this point, model explainability comes into play, as it helps the designer to make the best possible decisions as regards minimising the number of iterations needed to achieve the objective of fitting the *Port Area* values to the ML model.

In order to increase the area of Ports 1 and 2, it is necessary to change their geometry. The most common and simplest approach is, if possible, that of attempting to perform all port modifications without changing the position of the bridges. If the geometry of the ports is modified in this

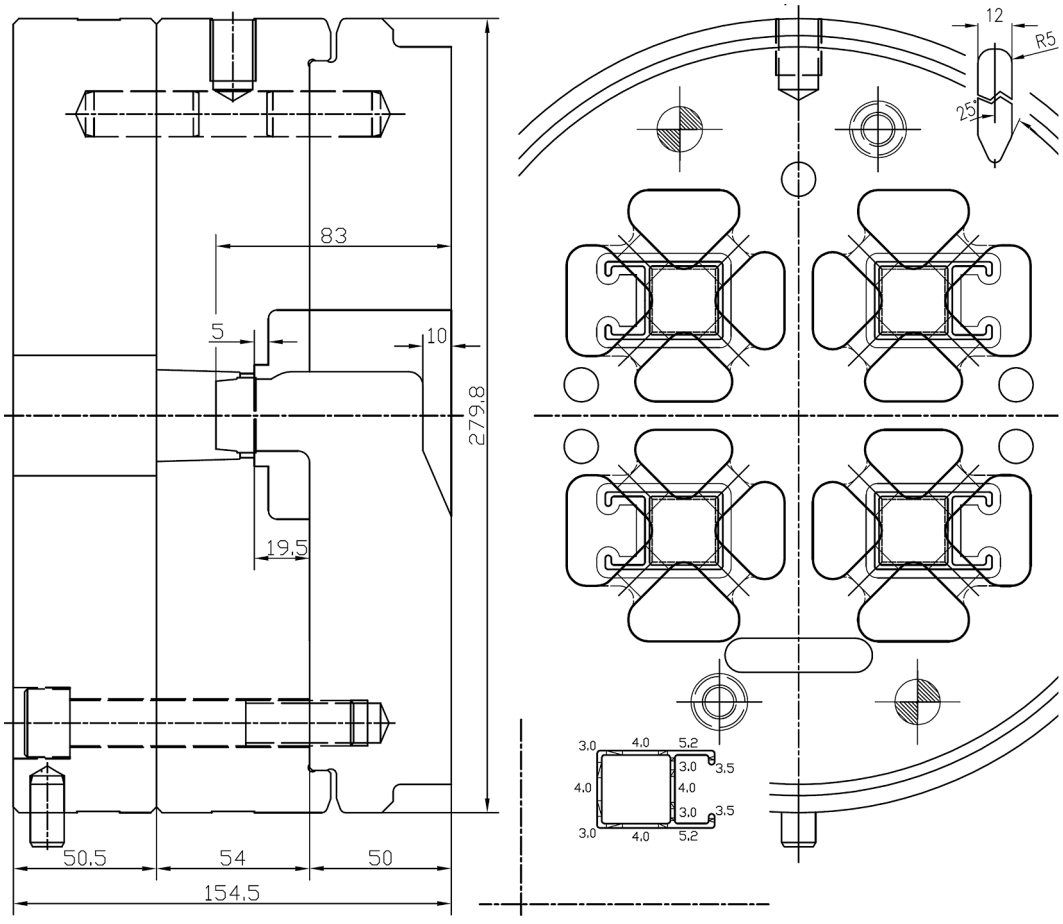

Fig. 19. Complete final die design.

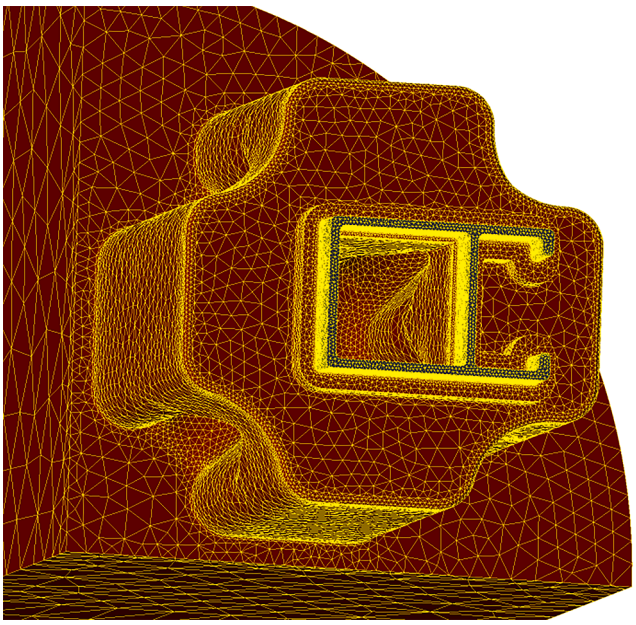

Fig. 20. Finite elements of the workpiece of final die design.

way, only the values of the variables *Total Port Area*, *Distance* and *Distance Port Profile* are altered.

Fig. 16 shows that *Total Port Area* contributes positively to the *Port Area* value of Ports 1 and 2, while *Distance* and *Distance Port Profile* contribute negatively.

Increasing the area of Ports 1 and 2 will always tend to increase *Total Port Area*, which in turn makes a positive contribution to the *Port Area*, regardless of the geometrical modification made in order to achieve such an increase.

This is not, however, the case of the variables *Distance* and *Distance Port Profile*. The change made to these variables may make it easier or less easy to achieve the final objective depending on how the *Port Area* is increased. If the decision is made to increase the *Port Area* by reducing the central wall of 10 mm, the value of *Distance* and *Distance Port Profile* will increase (especially the second one), and with it their negative contribution that reduces the *Port Area* value to which the model points (which is the exact opposite of the purpose of increasing the *Port Area*).

In the case of Ports 1 and 2, the decision was, therefore, made to increase the *Port Area* by reducing only the fillet radius, signifying that an increase in *Port Area* is achieved with practically no change in *Distance* and *Distance Port Profile*.

However, Ports 3 and 4 must be reduced in area. Fig. 16 shows that for these ports, the contributions of *Distance* and *Total Port Area* are positive while the contribution of *Distance Port Profile* is negative (and much smaller than the previous ones).

In this case, the decision was, therefore, made to modify the areas by stretching the geometry and reducing the *Port Area*, *Total Port Area* and *Distance*. The contribution of *Total Port Area* and *Distance* is in the same direction as the modification made. In this case, the *Distance Port Profile* is also reduced and contributes slightly in the opposite direction to the intended modification.

The model's explainability and a simple two-step iterative process have helped make it possible to define new geometries for the ports in the example die that fit the ML-based model perfectly (Fig. 17).

For these improved geometries, the value of the variables involved in the ML-based model are given in Table 5. These values have been fed into the model in order to obtain the results shown in Fig. 18 and Table 6. These show the predictions obtained by the ML-based model, the RMSE value and the RMSE quantile.

This new design, therefore, allows all ports to fit into the ML-based model in an appropriate manner, and this port design can consequently be considered adequate.

Once the optimal port design has been reached, the remaining elements have to be defined to complete the design (Fig. 19). It is important that the choice during their definition follows standard criteria to ensure that the calculation of balanced ports is reflected in a balanced flow of aluminium during extrusion. The design factors defined and the criteria used are listed below:

1. The bridges are defined with the following geometrical characteristics:

Table 7
Values for the definition of the property functions of the aluminium alloy.

Temperature [°C]	Density [kg/m^3]	Specific Heat [J/(kg·K)]	Thermal Expansion [1/°C)]
20	2699	904	2.26·E-5
500	2586	1026	2.78·e-5
Temperature [°C]	**Thermal Conductivity [W/(m·K)]**	**Young Module [MPa]**	**Poisson Ratio**
20	205	70,600	0.33
500	247	46,000	0.36

Table 8
Coefficients used by Qform UK for the H-S model for 6063 aluminium alloy in °C.

Coefficient	Value	Coefficient	Value	Coefficient	Value
A [MPa]	265	m_1	−0.00458	m_2	−0.12712
m_3	0.12	m_4	−0.0161	m_5	0.00026
m_7	0	m_8	0	m_9	0

Table 9
Mechanical properties of AISI H-13 steel depending on temperature.

Temperature [°C]	Density [kg/m^3]
20	7716
100	7692
200	7660
800	7459
Temperature [°C]	**Yield Stress [MPa]**
20	1500
300	1300
500	1100
570	1020
Temperature [°C]	**Young Module [MPa]**
20	210,000
300	187,000
600	160,000

Table 10
Temperature and dimensions of tooling and billet.

	Temp (°C)	Diameter (mm)	Length (mm)
Container	420	in = 210 out = 900	1055
Billet	480	203	500
Ram	370	209	1254
Die ring	450	out = 530 in = 282	154
Backer	450	out = 280	50.5
Bolster	430	out = 530	250
Mandrel	450	out = 280	50
Die	450	out = 280	54

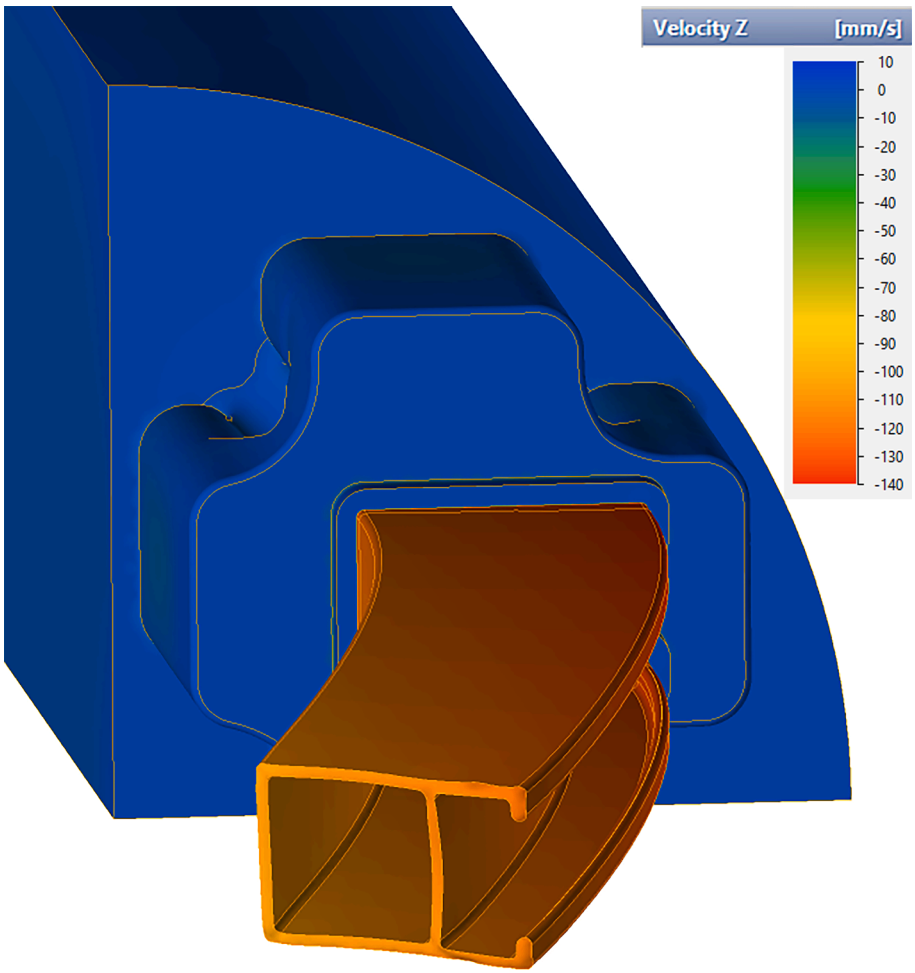

Fig. 21. Graphical representation of the Z-velocity (extrusion direction) for the initial unbalanced design.

- Width 12 mm. For this size of profile, the bridge widths are usually between 12 and 14 mm, a value was chosen that would allow the creation of fairly wide ports (which are more sensitive to flow imbalances).
- Welding angle 25 degrees. The welding angle values are usually between 20 and 30 degrees. An intermediate value is chosen, which favours welding and does not lengthen the welding distance too much (Valberg, 2002).

2. The welding chamber is defined with a depth of 14.5 mm and a 4x5mm feeder is also provided (usually to facilitate adjustment work during the life of the die). This welding height is a high value, given the width chosen for the bridges (Donati & Tomesani, 2005). This allows welding to be carried out without restrictions (Selvaggio et al., 2011) (Ceretti et al., 2009).
3. The bearing lengths are defined depending only on the thickness (in this case constant) and are reduced at the tips (Miles et al., 1997) and under the bridges (Xue et al., 2018).
4. Finally, the heights of the parts are defined on the basis of strength calculations to ensure adequate longevity under the cyclical conditions of pressure and temperature that they must withstand.

5.2. Verification of the example with FEM simulation

In order to validate the predictions of the ML-based model, they are compared with the predictions of the numerical simulation using the Qform UK software from Micas Simulations Ltd. This is specific-purpose software for simulation of metal deformation processes based on the finite element method and the Lagrange-Euler approach. This software allows an analysis of the material flow coupled to the mechanical deformations and stresses supported by the tool set, which helps to achieve a high accuracy of the numerical results (Biba et al., 2012). The numerical calculation considers the important influence that the die deformation has on the material flow through the die.

The FEM model of the workpiece flow domain is shown in Fig. 20. A quarter model is created owing to the symmetry of the design geometry. This domain represents the volume of extruded metal filling the interior space of the die set and the container.

All meshes are created with tetrahedral elements. A highly adaptive meshing is applied in order to optimise mesh quality and minimise the resources required to achieve accurate calculation results. The size of the elements in each zone is determined according to the extent of local deformation undergone during the process.

The billet material is EN AW-6063-O aluminium alloy and the die material is AISI H-13 steel. All the properties of these materials are temperature-dependent functions.

With regard to 6063 aluminium alloy, density, specific heat, thermal expansion, thermal conductivity, Young's modulus and Poisson's ratio are defined by employing a linear temperature-dependent function. Qform UK uses the values shown in Table 7 for the definition of the property functions of the aluminium alloy.

There are different models that can be used with the aim of modelling the flow stress of aluminium during the extrusion process. Of all the possible models, the International Conference on Extrusion and Comparison (ICEB) advocates the utilisation of the Hansel-Spittel (H-S)

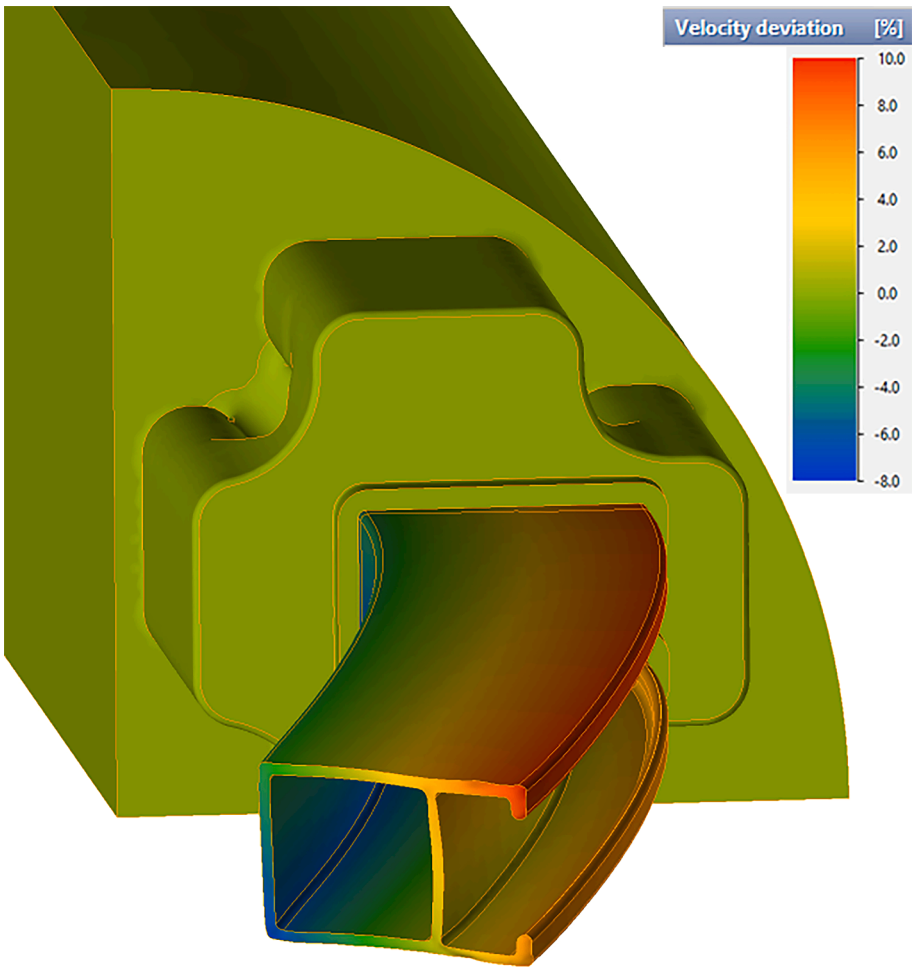

Fig. 22. Graphical representation of the velocity deviation for the initial unbalanced design.

model (3). The H-S model is used to represent the flow stress, and its dependence on strain is also considered. The H-S model function is derived by regressing the experimental data obtained from hot torsion tests (Gamberoni et al., 2015).

$$\sigma = A \bullet e^{m_1 T} \bullet T^{m_9} \bullet \varepsilon^{m_2} \bullet e^{m_4/\varepsilon} \bullet (1+\varepsilon)^{m_5 T} \bullet e^{m_7 \varepsilon} \bullet \varepsilon^{m_3} \bullet \varepsilon^{m_8 T} \quad (3)$$

The H-S model can be performed with a maximum number of 9 regression coefficients (A and m_1 to m_9). ICEB recommends regression with at least 6 coefficients so as to avoid a low correlation R^2 index. The coefficients are obtained from experimental torque test values. In order to cover all possible conditions, tests should be performed at different temperatures and strain velocities. The coefficients used by Qform UK for the flow stress model of 6063 aluminium alloy are shown in Table 8.

The AISI H-13 steel in the die is considered to be an elastic–plastic continuum subjected to small deformations. Table 9 shows the values used by Qform UK to generate the mechanical property functions of the material.

Poisson's ratio for steel is 0.3 for this alloy and is independent of temperature. In the contact areas between aluminium and steel the heat exchange coefficient is 30000 W/(m^2·K).

The friction of aluminium on steel in the extrusion temperature range is usually modelled as complete sticking. Only in the bearing zones is some sliding considered. ICEB suggests using a simple shear friction model (4) with m = 1 (Donati et al., 2019):

$$\tau = m \cdot \tau_s \quad (4)$$

where τ - shear friction stress

m - friction factor

τ_s - material shear stress

Qform UK models the friction between the aluminium and the die surface using the friction model proposed by Levanov (1997):

$$f_\tau = m \bullet \overline{\sigma} \Big/ \sqrt{3}\,[1 - \exp(-1.25 \bullet \sigma_n/\overline{\sigma})] \quad (5)$$

where σ_n - normal contact pressure

m - friction factor

The Levanov model (5) can be considered as a combination of the Coulomb friction model and the constant friction model. For low contact pressure, it provides a frictional traction that depends linearly on the normal contact stress. However, for a high contact pressure value, it provides a similar level of frictional traction as the constant friction model.

Table 10 shows the main boundary conditions, dimensions and temperature parameters of the extrusion process used in the Qform UK FEM simulation.

Moreover, it is important to note that a profile speed similar to those commonly used in real extrusion tests in the press has been used as a velocity condition for the simulation of the process (Engelhardt et al., 2019).The most common practice for non-special profiles is that of

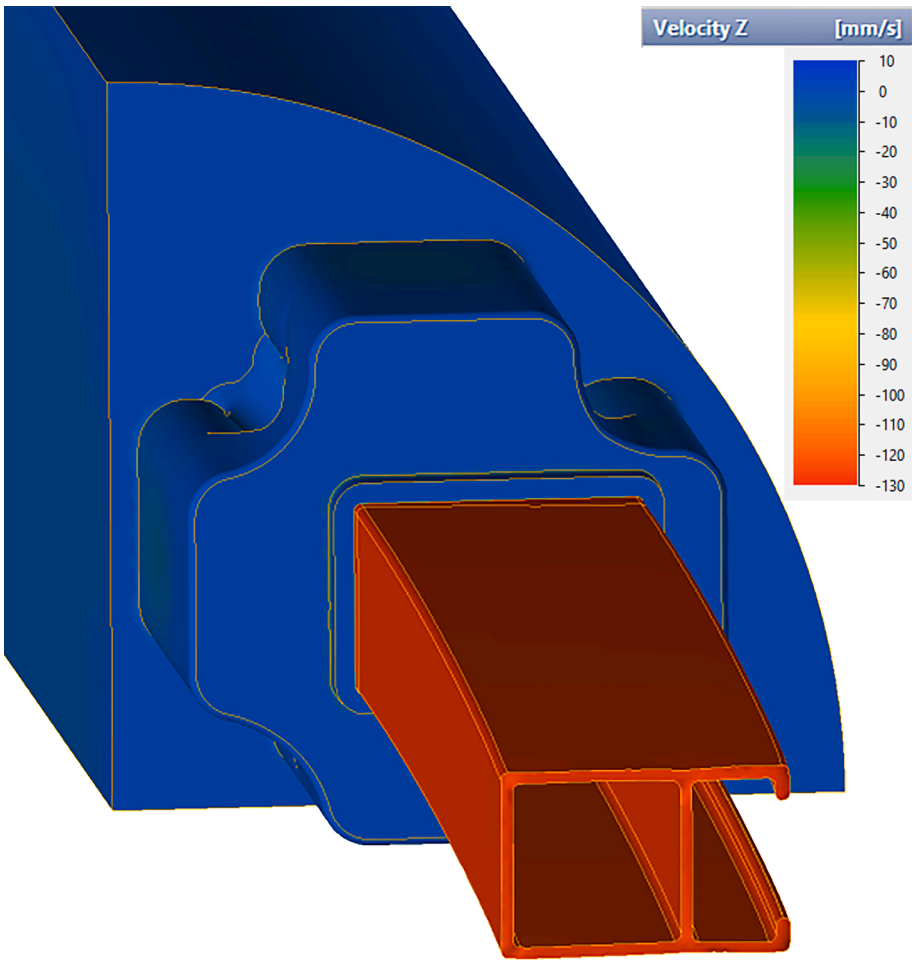

Fig. 23. Graphical representation of the Z-velocity (extrusion direction) for the final balanced design.

employing velocities between 100 and 180 mm/s at the press output. An exit velocity value of 133 mm/s has been used for the FEM simulations in this study.

Bearing all of the above-mentioned boundary conditions and criteria in mind, two FEM simulations of the extrusion were performed using the Qform UK: a first simulation of the initial unbalanced design and a second simulation of the design obtained after the application of the ML-based model.

The simulation results for the velocity in the extrusion direction for the initial unbalanced design are shown in Fig. 21. An unbalance of the Z-velocity will be noted which causes a profile deviation from that direction.

The results of the velocity deviation for the initial unbalanced design with respect to its average velocity are shown in Fig. 22. The chromatic scale in the figure reveals that the range of the velocity deviation at the exit of the press is around 18% between the fastest and the slowest zones.

A speed difference of this magnitude at the exit from the press always results in a deformation of the profile and, in most cases, in the deflection of the mandrel. In the vast majority of cases, mandrel deflections also produce differences in thickness in the hollow portions of the profile.

Determining the maximum admissible velocity deviation at the exit of the press for each specific profile can be very difficult. In order to extrude a profile according to the manufacturing tolerances, the maximum range for the velocity deviation depends on several factors. These factors include: the stiffness of the profile as a result of its shape, the general thickness of the profile, specific tolerances for the profile, etc… But it is widely recognised that minimising the velocity range always helps to guarantee a profile that is geometrically closer to that desired.

Fig. 23 shows the Z-velocity results, while Fig. 24 shows the velocity deviation for the final balanced design using the ML-based model. The chromatic scale in the figure reveals that the range of the velocity deviation at the exit of the press is around 1.9% between the fastest and the slowest zones.

Nodal results and animations of the different simulations carried out using Qform UK can be found in the dataset associated with this paper (Llorca-Schenk, 2022).

A comparative analysis of the velocity deviation values of the design obtained with the help of the ML-based model and the previous linear regression-based model reveals that the results of the new model are considerably better than those of the previous model (Fig. 25) (Table 11). It achieves a substantial reduction of 15% in the velocity deviation range that was observed in the design obtained from the linear regression-based model (Llorca-Schenk et al., 2021).

Despite being an example profile for which the linear regression-based model achieves a very acceptable modelling, the new ML-based model achieves an important improvement, probably owing to the fact that it manages to extract the existing non-linear relationships between the variables that were ignored by the linear model.

The other common and complementary means employed to evaluate the goodness of the extrusion simulation results is to employ the sum of squares of the nodal values of the velocity deviation from its mean value

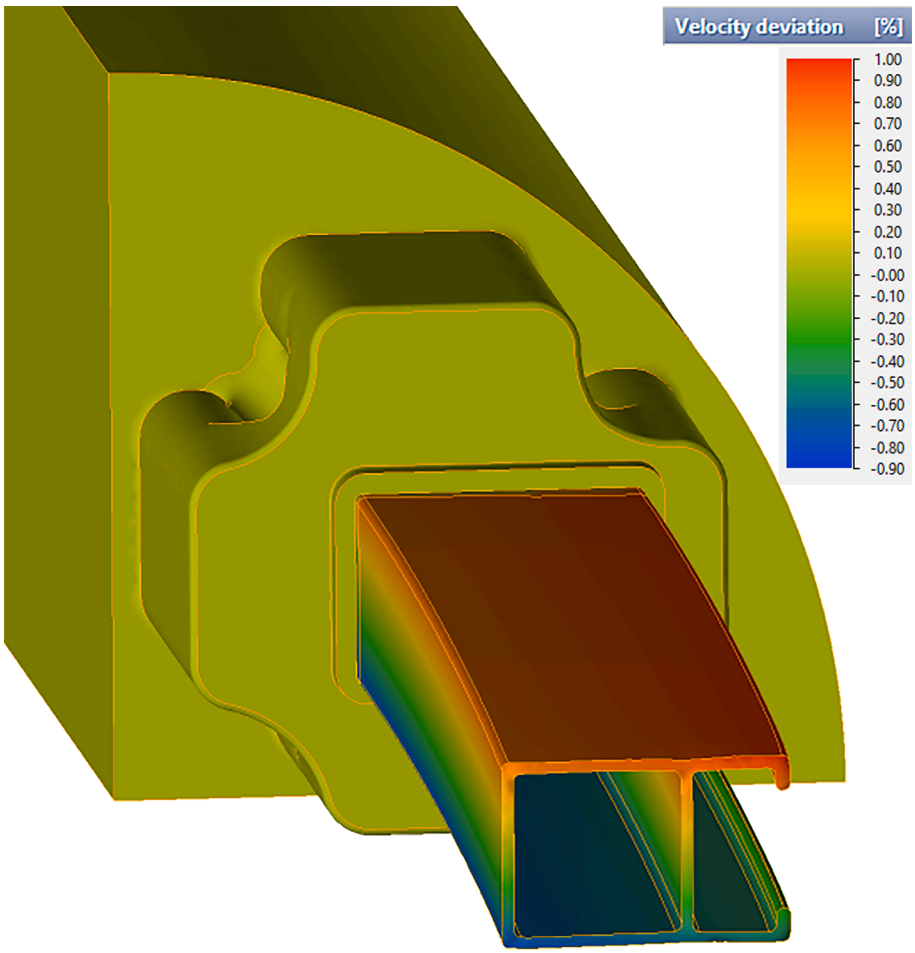

Fig. 24. Graphical representation of the velocity deviation for the final balanced design.

or RMSD (root mean square deviation). Evaluating the square deviation makes it possible to assess the goodness of the results in the entire profile section, and not by simply focusing on the extremes of the velocity deviation range.

This analysis is always carried out by starting from the bearing zone, as the profile has not yet been formed in the aluminium zone before the bearing. In the specific case of this evaluation of the square deviation, the nodal values of the first 100 mm of the shaped profile from the bearing are considered (which corresponds to more than 100,000 nodes).

According to the goodness analysis shown throughout this section, the new ML-based model obtains comparatively much better results than the linear regression-based model. This indicates that, beyond a substantial improvement to the reduction in the extreme values of velocity deviation, there is a noticeable improvement in the prediction of the flow of the aluminium through the whole profile section (Table 12).

This considerable improvement has even been shown through an example which, given its characteristics, had already achieved very good results when compared to the previous linear regression-based model. This suggests that, in the case of profiles that are more difficult for the regression-based model to deal with, it is very plausible that the enhancement obtained by considering its non-linearities could be even greater.

6. Conclusions and future research

The procedure developed in order to obtain the ML-based model with which to design the ports of porthole aluminium extrusion die has, in general terms, attained successful results. The new ML-based model can significantly facilitate the design process of such die ports, particularly because it can provide the designer with essential support at the beginning of the creation process.

The ML-based model is a means to summarise the experience and know-how developed through a large number of optimal designs over time. In addition, given the characteristics of the model, it makes it easy to add new experiences to the model, and it can, therefore, easily learn from new designs.

It is suitable for a specific type of very common dies: four-cavity dies with four ports per cavity. In the case of other dies with other geometrical configurations, it will be necessary to obtain new models or a general model in the future.

When compared to the previous linear regression-based model, the new ML-based model achieves a substantial reduction in the velocity deviation in the profile section when the design obtained by the model is analysed by employing FEM simulation.

Moreover, the explainability of the ML-based model makes it possible to discover the magnitude and direction of the relative influence of each of the variables in a given case. This greatly facilitates decision-making regarding the modifications to be made in order to adjust an initial design to the ML-based model. The improvement in the results and the facilities for design correction provided by explainability suggest that the level of requirement in the reduction of velocity deviation in the final design may achieve values that it has been difficult to imagine until now.

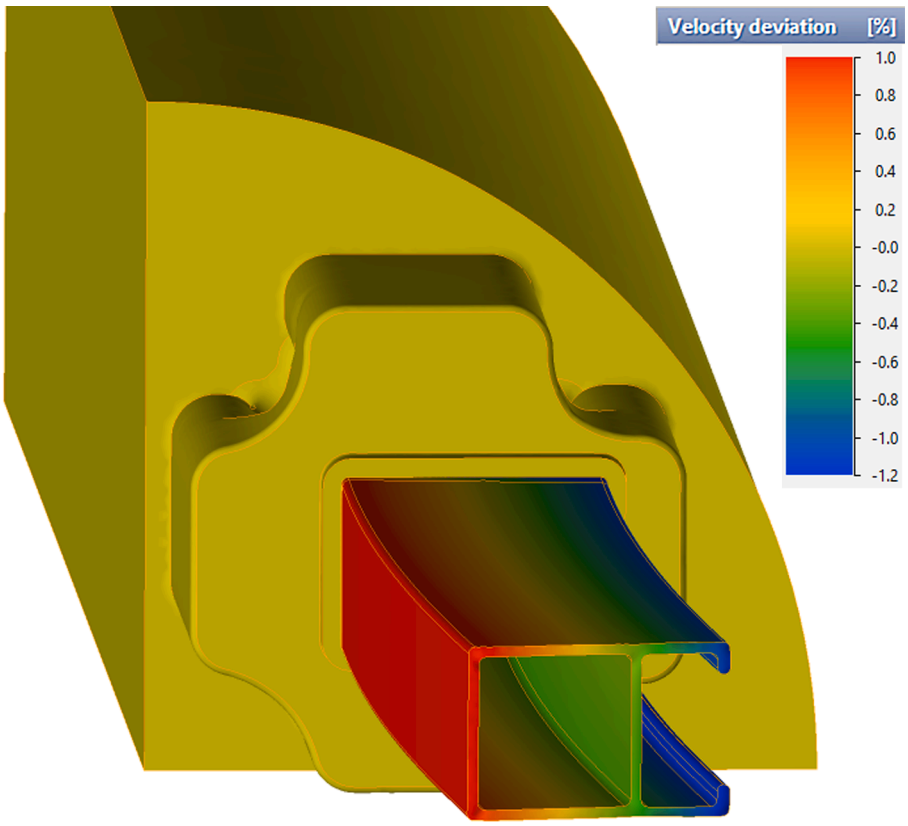

Fig. 25. Velocity deviation for the balanced design obtained with the previous linear regression-based model.

Table 11
Comparison of the most important variables obtained in the optimal design achieved with the help of the new ML-based model and the previous linear regression-based model (Llorca-Schenk et al., 2021).

Port	ML Port Area (mm^2)	Linear Port Area (mm^2)	ML Distance (mm)	Linear Distance (mm)	ML Total Port Area (mm^2)	Linear Total Port Area (mm^2)
1	610.16	599.59	43.2	43.17	11585.76	11454.58
2	610.16	599.59	43.2	43.17	11585.76	11454.58
3	879	867.32	80.59	80.46	11585.76	11454.58
4	797.12	797.12	79.63	79.63	11585.76	11454.58

Table 12
Values of the root mean square deviation from bearing zone onwards.

	Unbalanced design	Balanced design bylinear regression-based model (Llorca-Schenk et al., 2021)	Balanced design by ML-based model
Mean nodal velocity deviation (m/s)	0.00618	0.00115	0,000745
Sum of squares of nodal velocity deviation (m^2/s^2)	274.57	5.53	1,95
Root main square deviation – RMSD (m/s)	16.57	2.35	1,39

Given the geometric linkage between the different variables involved in the model, it is currently not possible to use it for the creation of a new design from scratch. One possible means of future development is also open in the sense of overcoming the limitation of using it only for design checking. An attempt could be made to define a tool that would make it possible to automate the calculation and iterative modification of the initial design until a new final port design adjusted to the model is obtained. This new tool could probably be articulated around a parametric CAD (Computer Aided Design) tool that iteratively and incrementally modifies the design until an optimal result is achieved for the calculation of the ML-based model.

Data availability

The raw data required to reproduce ML analysis and FEM simulation has been shared in Mendeley Data (Llorca-Schenk, 2022): https://doi.org/10.17632/dy97xr6t8h.1.

8. Role of the funding source

This research did not receive any specific grant from funding agencies in the public, commercial, or not-for-profit sectors.

The authors would like to thank Micas Simulations Ltd for licensing Qform UK for FEM verification.

CRediT authorship contribution statement

Juan Llorca-Schenk: Conceptualization, Methodology, Formal analysis, Investigation, Writing – original draft, Writing – review & editing, Project administration. **Juan Ramón Rico-Juan:** Writing – original draft, Data curation, Software, Validation. **Miguel Sanchez-Lozano:** Writing – review & editing, Supervision.

Declaration of Competing Interest

The authors declare that they have no known competing financial interests or personal relationships that could have appeared to influence

the work reported in this paper.

Acknowledgements

This work was partially supported by the DIDET Group (Diseño en Ingeniería y Desarrollo Tecnológico) at the University of Alicante (UA VIGROB-032).

The authors thank the company HAEP, S.A. (Hydro Aluminium Extrusion Portugal) for enabling and facilitating access to information on the performance of the dies during extrusion.

References

Arif, A. F. M., Sheikh, A. K., & Qamar, S. Z. (2003). A study of die failure mechanisms in aluminum extrusion. *Journal of Materials Processing Technology, 134*(3), 318–328. https://doi.org/10.1016/S0924-0136(02)01116-0

Barredo Arrieta, A., Díaz-Rodríguez, N., Del Ser, J., Bennetot, A., Tabik, S., Barbado, A., … Herrera, F. (2020). Explainable Artificial Intelligence (XAI): Concepts, taxonomies, opportunitiesinable and challenges toward responsible AI. *Information Fusion, 58*, 82–115. https://doi.org/10.1016/j.inffus.2019.12.012

Biba, N., Stebunov, S., & Lishny, A. (2012). The model for coupled simulation of thin profile extrusion. *Key Engineering Materials, 504–506*, 505–510. https://doi.org/10.4028/www.scientific.net/KEM.504-506.505

Breiman, L. (2001). Random forests. *Machine Learning, 45*(1), 5–32. https://doi.org/10.1023/A:1010933404324

Breiman, L., Friedman, J. H., Olshen, R. A., & Stone, C. J. (1984). *Classification and regression trees*. Routledge. https://doi.org/10.1201/9781315139470.

Ceretti, E., Fratini, L., Gagliardi, F., & Giardini, C. (2009). A new approach to study material bonding in extrusion porthole dies. *CIRP Annals - Manufacturing Technology, 58*(1), 259–262. https://doi.org/10.1016/j.cirp.2009.03.010

Chen, T., & Guestrin, C. (2016). XGBoost: A scalable tree boosting system. *Proceedings of the ACM SIGKDD International Conference on Knowledge Discovery and Data Mining, 13–17*, 785–794. https://doi.org/10.1145/2939672.2939785.

Chen, T. H., & Chang, R. C. (2021). Using machine learning to evaluate the influence of FinTech patents: The case of Taiwan's financial industry. *Journal of Computational and Applied Mathematics, 390*, Article 113215. https://doi.org/10.1016/j.cam.2020.113215

Cortes, C., & Vapnik, V. (1995). Support-vector networks. *Machine Learning, 20*, 273–297. https://doi.org/10.1023/A:1022627411411

Cover, T. M., & Hart, P. E. (1967). Nearest neighbor pattern classification. *IEEE Transactions on Information Theory, 13*(1), 21–27. https://doi.org/10.1109/TIT.1967.1053964

Dalzochio, J., Kunst, R., Pignaton, E., Binotto, A., Sanyal, S., Favilla, J., & Barbosa, J. (2020). Machine learning and reasoning for predictive maintenance in Industry 4.0: Current status and challenges. *Computers in Industry, 123*, Article 103298. https://doi.org/10.1016/j.compind.2020.103298

Donati, L., Segatori, A., Gamberoni, A., Reggiani, B., & Tomesani, L. (2019). Extrusion benchmark 2017: Effect of die design on profile quality and distortions of thin C-shaped hollow profiles. *Materials Today: Proceedings, 10*(2), 171–184. https://doi.org/10.1016/j.matpr.2018.10.394

Donati, L., & Tomesani, L. (2004). The prediction of seam welds quality in aluminum extrusion. *Journal of Materials Processing Technology, 153–154*, 366–373. https://doi.org/10.1016/j.jmatprotec.2004.04.215

Donati, L., & Tomesani, L. (2005). The effect of die design on the production and seam weld quality of extruded aluminum profiles. *Journal of Materials Processing Technology*. https://doi.org/10.1016/j.jmatprotec.2005.02.156

Dorogush, A. V., Ershov, V., & Gulin, A. (2018). CatBoost: Gradient boosting with categorical features support. *ArXiv*. http://arxiv.org/abs/1810.11363.

Engelhardt, M., Kurmajev, S., Maier, J., Becker, C., & Hora, P. (2019). The application of FEA for optimization of die design. *Materials Today: Proceedings, 10*(2), 226–233. https://doi.org/10.1016/j.matpr.2018.10.400

Freund, Y., & Schapire, R. E. (1997). A decision-theoretic generalization of on-line learning and an application to boosting. *Journal of Computer and System Sciences, 55*(1), 119–139. https://doi.org/10.1006/jcss.1997.1504

Gamberoni, A., Donati, L., Reggiani, B., Haase, M., Tomesani, L., & Tekkaya, A. E. (2015). Industrial benchmark 2015: process monitoring and analysis of hollow EN AW-6063 extruded profile. *Materials Today: Proceedings, 2*(10), 4714–4725. https://doi.org/10.1016/j.matpr.2015.10.004

Giarmas, E., & Tzetzis, D. (2022). Optimization of die design for extrusion of 6xxx series aluminum alloys through finite element analysis: A critical review. *International Journal of Advanced Manufacturing Technology, 119*, 5529–5551. https://doi.org/10.1007/s00170-022-08694-3

He, Z., Wang, H. N., Wang, M. J., & Li, G. Y. (2012). Simulation of extrusion process of complicated aluminium profile and die trial. *Transactions of Nonferrous Metals Society of China (English Edition), 22*(7), 1732–1737. https://doi.org/10.1016/S1003-6326(11)61380-0

Hinton, G. E. (1989). Connectionist learning procedures. *Artificial Intelligence, 40*(1–3), 185–234. https://doi.org/10.1016/0004-3702(89)90049-0

Hoerl, A. E., & Kennard, R. W. (1970). Ridge regression: Biased estimation for nonorthogonal problems. *Technometrics, 12*(1), 55–67. https://doi.org/10.1080/00401706.1970.10488634

Ke, G., Meng, Q., Finley, T., Wang, T., Chen, W., Ma, W., … Liu, T. Y. (2017). LightGBM: A highly efficient gradient boosting decision tree. *Advances in Neural Information Processing Systems, 30*, 3149–3157.

Koh, P. W., & Liang, P. (2017). Understanding black-box predictions via influence functions. In *34th International Conference on Machine Learning, ICML 2017*, *4*, 2976–2987. https://doi.org/10.48550/arXiv.1703.04730.

Levanov, A. N. (1997). Improvement of metal forming processes by means of useful effects of plastic friction. *Journal of Materials Processing Technology, 72*(2), 314–316. https://doi.org/10.1016/S0924-0136(97)00191-X

Lin, C., & Ransing, R. S. (2009). An innovative extrusion die layout design approach for single-hole dies. *Journal of Materials Processing Technology, 209*(7), 3416–3425. https://doi.org/10.1016/j.jmatprotec.2008.07.042

Liu, B. (2021). New technology application in logistics industry based on machine learning and embedded network. *Microprocessors and Microsystems, 80*, Article 103596. https://doi.org/10.1016/j.micpro.2020.103596

Llorca-Schenk, J. (2022). Dataset for Designing extrusion dies on the basis of eXplainable Artificial Intelligence. *Mendeley Data, V1*. https://doi.org/10.17632/dy97xr6t8h.1

Llorca-Schenk, J., Sentana-Gadea, I., & Sanchez-Lozano, M. (2021). Design of porthole aluminium extrusion dies through mathematical formulation. *Materials Today Communications, 27*, Article 10231. https://doi.org/10.1016/j.mtcomm.2021.102301

Lucignano, C., Montanari, R., Tagliaferri, V., & Ucciardello, N. (2010). Artificial neural networks to optimize the extrusion of an aluminium alloy. *Journal of Intelligent Manufacturing, 21*, 569–574. https://doi.org/10.1007/s10845-009-0239-0

Lundberg, S. (2019). *SHAP (SHapley Additive exPlanations) [Computer software]*. Github Repository. https://github.com/slundberg/shap.

Lundberg, S. M., & Lee, S. I. (2017). A unified approach to interpreting model predictions. *Advances in Neural Information Processing Systems, 30*, 4766–4775. https://doi.org/10.48550/arXiv.1705.07874

Miles, N., Evans, G., & Middleditch, A. (1997). Bearing lengths for extrusion dies: Rationale, current practice and requirements for automation. *Journal of Materials Processing Technology, 72*(1), 162–176. https://doi.org/10.1016/S0924-0136(97)00150-7

Mori, T., Takatsuji, N., Matsuki, K., Aida, T., Murotani, K., & Uetoko, K. (2002). Measurement of pressure distribution on die surface and deformation of extrusion die in hot extrusion of 1050 aluminum rod. *Journal of Materials Processing Technology, 130–131*, 421–425. https://doi.org/10.1016/S0924-0136(02)00718-5

Narciso, D. A. C., & Martins, F. G. (2020). Application of machine learning tools for energy efficiency in industry: A review. *Energy Reports, 6*, 1181–1199. https://doi.org/10.1016/j.egyr.2020.04.035

Pietzka, D., Ben Khalifa, N., Donati, L., Tomesani, L., & Tekkaya, A. E. (2009). Extrusion benchmark 2009 experimental analysis of deflection in extrusion dies. *Key Engineering Materials, 424*, 19–26. https://doi.org/10.4028/www.scientific.net/kem.424.19

Roth, A. E. (1988). *The shapley value : essays in honor of LLoyd S. Shapley* (1st Ed.). Cambridge University Press.

Saha, P. K. (2000). Extrusion die and tooling. In *Aluminum extrusion technology* (1st Ed., pp. 87–118). ASM International. https://doi.org/10.31399/asm.tb.aet.t68260087.

Schikorra, M., Donati, L., Tomesani, L., & Tekkaya, A. E. (2008). Extrusion benchmark 2007 – Benchmark experiments: study on material flow extrusion of a flat die. *Key Engineering Materials, 367*, 1–8. https://doi.org/10.4028/www.scientific.net/kem.367.1

Selvaggio, A., Kloppenborg, T., Schwane, M., Hölker, R., Jäger, A., Donati, L., … Tekkaya, A. E. (2013). Extrusion benchmark 2013 - Experimental analysis of mandrel deflection, local temperature and pressure in extrusion dies. *Key Engineering Materials, 585*, 13–22. https://doi.org/10.4028/www.scientific.net/kem.585.13

Selvaggio, A., Segatori, A., Güzel, A., Donati, L., Tomesani, L., & Tekkaya, A. E. (2011). Extrusion benchmark 2011: Evaluation of different design strategies on process conditions, die deflection and seam weld quality in hollow profiles. *Key Engineering Materials, 491*, 1–10. https://doi.org/10.4028/www.scientific.net/KEM.491.1

Sharma, A. (2018). Guided Stochastic Gradient Descent Algorithm for inconsistent datasets. *Applied Soft Computing Journal, 73*, 1068–1080. https://doi.org/10.1016/j.asoc.2018.09.038

Tibshirani, R. (1996). Regression shrinkage and selection via the lasso. *Journal of the Royal Statistical Society: Series B (Methodological), 58*(1), 267–288. https://doi.org/10.1111/j.2517-6161.1996.tb02080.x

Valberg, H. (2002). Extrusion welding in aluminium extrusion. *International Journal of Materials and Product Technology, 17*(7), 497–556. https://doi.org/10.1504/ijmpt.2002.001317

Wilcoxon, F. (1945). Individual comparisons by ranking methods. *Biometrics Bulletin, 1*(6), 80–83. https://doi.org/10.2307/3001968

Xue, X., Vincze, G., Pereira, A. B., Pan, J., & Liao, J. (2018). Assessment of metal flow balance in multi-output porthole hot extrusion of AA6060 thin-walled profile. *Metals, 8*(6), Article 462. https://doi.org/10.3390/met8060462.

Yan, H., & Xia, J. (2006). An approach to the optimal design of technological parameters in the profile extrusion process. *Science and Technology of Advanced Materials, 7*(1), 127–131. https://doi.org/10.1016/j.stam.2005.11.017

Yu, J., Zhao, G., Cui, W., Chen, L., & Chen, X. (2019). Evaluating the welding quality of longitudinal welds in a hollow profile manufactured by porthole die extrusion: Experiments and simulation. *Journal of Manufacturing Processes, 38*, 502–515. https://doi.org/10.1016/j.jmapro.2019.01.044

Zhu, H., Couper, M. J., & Dahle, A. K. (2011). Effect of process variables on Mg-Si particles and extrudability of 6xxx series aluminum extrusions. *JOM, 63*, 66–71. https://doi.org/10.1007/s11837-011-0183-2